Abstract

This thesis describes a psychophysical experiment carried out to assess the perceptual influence of approximating ambient occlusion in real-time rendering. Three different screen-space ambient occlusion techniques of differing physical accuracy were implemented for the experiment. The results of the experiment show that screen-space ambient occlusion can increase the perceived realism of visually complex synthetic images. Visual complexity was also found to have an influence on the required physical accuracy of the ambient occlusion algorithm. Specifically, as the visual complexity increases, the required physical accuracy of ambient occlusion decreases. In a visually complex, ecologically valid scenario, experiment participants were not able to discern a difference between two different screen-space ambient occlusion techniques with significant observable quality differences. The results of the experiment suggest that in practical application scenarios such as computer games, it is prudent to investigate the need for, and impact of, screen-space ambient occlusion for individual scenes or environments. In many cases, low accuracy ambient occlusion can be sufficient, and in some cases it can be turned off completely; thus allowing for more computation time to be utilized on other perceptually important rendering tasks.

This page is intentionally left blank

Preface

This thesis was made at Aalborg University Copenhagen in fulfilment of the requirements for acquiring the Master of Science degree in Medialogy, M.Sc. Medialogy. Work on the thesis was carried out over a period of four months constituting a full semester and 30 ECTS points.

The contents of the thesis constitute advanced topics in computer graphics programming and so it is assumed that the reader possesses knowledge comparable to a bachelor in Computer Science.

The thesis comes with a CD holding this report and appendix materials that are not included in the printed appendix (such as code and stimuli images). The CD contains a readme file explaining the file structure and all the contents included.

The thesis is divided into six distinct chapters. The first chapter constitutes the introduction and outlines the background of the thesis as well as the motivation and goal. Chapter 2 describes work relevant for the thesis, while chapter 3 covers the theory necessary for carrying out the implementation detailed in chapter 4. Chapter 5 covers the details of setting up and carrying out a psychophysical experiment while chapter 6 rounds up the thesis with a discussion and conclusion.

Aalborg University Copenhagen, May 2010

Christian Jakobsen

Acknowledgements

I would like to thank Daniel Grest for supervision and guidance; Crytek GmbH for creating the Sponza model and textures used in the experiment and making it available to the general public; and both Crytek and Blizzard Entertainment for making their ambient occlusion algorithms available to the public.

Table of Contents

Chapter 1: Introduction

Striving for realism in real-time rendering is a difficult proposition at best. The amount of calculations required to match how light interacts in the real world is staggering and completely impractical for real-time purposes. Even in off-line rendering scenarios such as film and television production, where several hours or more can be dedicated to rendering a single frame of animation, approximations to how light behaves are often preferred in lieu of physical accuracy in order to cut down on rendering time. For example, ILM adapted an approach developed for real-time rendering as part of their global illumination pipeline in production of Pirates of the Caribbean (Robertson 2006). The use of approximations is of course even more relevant in real-time rendering scenarios where the time to render a single frame is reduced to a scale of milliseconds. Until recently, lighting in real-time rendering scenarios such as computer games has consisted of local illumination models only, with global illumination effects such as visibility determination and indirect light transport either being omitted, or pre-computed using techniques such as light maps and occlusion maps.

When using local illumination models in rendering, light is emitted from a light source and only surfaces that are directly visible from the light source are illuminated. In the real world, some of the light would be reflected or transmitted and proceed to illuminate other surfaces in the environment. This indirect light transport is a very important element of convincingly lighting a synthetic scene, but is unfortunately also a prohibitively expensive process for real-time rendering. Methods such as photon mapping (Jensen 1996) and radiosity (Goral, et al. 1984) are popular solutions in offline rendering scenarios, but graphics hardware have not yet progressed to the point where such solutions are feasible for time-critical applications such as computer games. Instead, these techniques are often employed as a pre-processing step, computed and stored in a light map which is later used in real-time to modulate the illumination a surface receives. This is a common trend, to approach the problem of global illumination in a piecemeal fashion, using a divide and conquer approach to

separate the complex problem of calculating the global illumination in a synthetic scene into smaller, more manageable problems. For example, using radiosity to calculate a light map only accounts for inter-diffuse reflections, but not other global illumination phenomena such as caustics and shadows. An important step that is omitted here is visibility determination which evaluates whether or not a shaded point can see another point and consequently, whether any indirect illumination should be calculated between those two points.

With the rapid increase in computing power offered by newer generations of graphical processing units, developers and academics alike have seen the possibilities of developing and implementing ever more flexible and accurate approximations to isolated global illumination phenomena. The research into this area can roughly be divided into two major categories; algorithms that work in object-space, and algorithms that work in screen-space. Techniques falling into the former category usually employ ray-tracing and full knowledge of the scene structure to calculate the light transport in a given scene, and have recently progressed into the realm of interactive frame rates, e.g. (Wang, et al. 2009). While this is an area of research that hold exiting potential for future applications; graphics hardware have not yet progressed to the point where such implementations can offer sufficient frame rates for more time critical applications such as computer games.

On the other hand, the category of screen-space approaches offers much faster techniques, operating only on visible pixels that have passed the depth test making it largely independent of scene complexity. Working on a limited data set instead of the full scene structure of course implies that techniques performed in screen-space are more coarse approximations of the real-world phenomena. A recent technique that have become popular in both literature and the computer games industry, commonly referred to as “Screen-Space Ambient Occlusion”, make some clever assumptions regarding how much indirect diffuse light a sample point is receiving based on nearby surrounding geometry. The result of applying ambient occlusion to indirect lighting is a darkening of areas where there is a lot of surrounding geometry. This provides

important perceptual cues regarding scene depth in the form of contact shadows (see figure 1); together with shading, shadows are a key component in the perceptual process of recovering depth information in a 2D image (Palmer 1999).

Figure 1 – Important depth cues are provided using ambient occlusion; the left image is shown without ambient occlusion and the right image is shown with ambient occlusion. Notice the shadows underneath the furniture and the much improved depth and surface detail of the plants.

Using screen-space ambient occlusion to modulate an indirect light contribution is a coarse approximation of real-world indirect light transport and is certainly not physically accurate. Even using ray-tracing with a large number of rays to calculate ambient occlusion is still an approximation, although a much finer one than the approach of calculating it in screen space. As a result, one could be tempted to disregard the technique when striving for realism in rendering, but ambient occlusion has been shown to provide perceptually plausible results both in real-time as well as off-line rendering scenarios.

1.1 Screen-Space Ambient Occlusion and Perceived Realism

While not the first to implement screen-space ambient occlusion, the technique used in Crytek's first-person shooter *Crysis* (Mittring 2007) was certainly the catalyst for an explosive increase in research in the area. Crytek's implementation is a rather crude approximation when compared to more accurate visibility determination using e.g. ray-tracing, and have since its inception endured some critique regarding its visual artefacts and seen many improvements and refinements from academics and

professionals alike. However, even three years past its release date, *Crysis* is arguably still one of the best looking computer games on the market. The superlative visuals presented in *Crysis* is of course not only due to the ambient occlusion technique used, but it does highlight an important realization that holds both for real-time and off-line rendering scenarios; physical accuracy of a rendering algorithm is not always a necessity for achieving perceptually plausible results (see figure 2). Actual perceived realism by an observer is much more important than any physical or numerical accuracy, and this makes screen-space approaches both viable and intriguing tools for calculating global illumination phenomena in real-time rendering scenarios, right now and for the foreseeable future.

Figure 2: Spectacular visuals from the computer game Crysis. Screen-Space ambient occlusion is in effect here and is adding depth to the foliage in particular.

A perhaps even more important consideration is that physical accuracy in rendering is not always the most desirable goal to strive for. While it makes intuitive sense to try and mimic the real-world as close as possible to improve rendering quality, there is no guarantee that this approach will result in a more perceptually plausible result. This notion is embodied in the area of research called perceptually-based rendering

(McNamara 2001). Perceptually-based rendering methods attempt to exploit the limitations of the human visual system to speed up rendering algorithms. Conceptually, the idea is to identify areas of high perceptual saliency in a synthetic image and focus computational power on these areas thus improving rendering quality by maximizing the time dedicated to perceptually important areas of the image. Whether this approach is consciously followed from a development point of view or not, the idea is often the basis for real-time rendering algorithms; born out of shear necessity for attaining real-time frame rates. The validity of a perceptually based approach is often determined either by using the visual difference predictor (Daly 1993) or a similar algorithm to map out the overall perceivable pixel error of the rendered image; or by conducting a psychophysical study on human observers comparing images side by side. For an example of both see (McNamara 2006). Either approach presupposes a *ground truth* or a *gold standard* image to which the approximation is compared.

While a comparative study of selective renderings and a real world or synthetic ground truth reference image can state a lot about the physical accuracy of a given rendering algorithm, it does not necessarily reveal anything useful about how *perceptually* realistic an image produced by a given algorithm is. In addition, the ground truth comparative study scenario is an inherently contrived experimental scenario that essentially has no real world correlate, that is to say; when experiencing computer generated imagery, whether it be in a movie or computer game or some other source, we rarely have a reference on hand to compare the realism of the displayed images with. One notable exception to this is the compositing of live action footage and computer generated imagery in film and television. In this case, it can make sense to attempt to maximize physical accuracy of the rendering algorithms used, since the final rendered images has to match the live action footage in quality and appearance. In real-time rendering scenarios there is no such comparison taking place, and the final arbiter on realism or rendering quality is how it is perceived by a human observer alone, not how it compares to real footage.

1.2 Thesis Motivation and Goal

This thesis is partly motivated by the observation that visibility approximations such as ambient occlusion have been shown to provide perceptually realistic results despite showing clear perceptible differences to "ground truth" reference images (Yu, et al. 2009). Additionally, as mentioned in the previous section ambient occlusion has become a popular topic in contemporary real-time rendering scenarios, especially computer games; but it is not clear what the perceptual influence of ambient occlusion is on perceived realism.

The aim of the thesis is to conduct a formal study into the perceptual characteristics of approximating global illumination phenomena in screen-space. More specifically, the goal of the study is to measure the effect of screen-space ambient occlusion on the perceived realism of a synthetic image. In order to make the subject amenable for experimental testing, the focus of the study is limited to visibility approximations in screen-space.

The main contribution of the thesis is a psychophysical study into the perceptual influence of using screen-space ambient occlusion in a real-time rendering context. In the literature, several studies have set out to measure the perceived realism of synthetic images created using different rendering algorithms (Yu, et al. 2009) (Sundstedt, et al. 2007) (Kozlowski and Kautz 2007) (Jimenez, Sundstedt and Gutierrez 2009), however, no such investigations have yet been carried out on the perceptual influence of screen-space ambient occlusion. Moreover, many perceptual studies involve experiments revolving around the ground truth reference scenario, where stimuli sets are subject to direct comparison. This study takes a different approach in an effort to map out the perceptual influence of screen space ambient occlusion in a more ecologically valid context; by carrying out a no-reference experiment with visually complex stimuli. The no-reference experiment denotes a comparison task between two images where no direct comparison is allowed, i.e. subjects are not allowed to view images side by side or flip back and forth between them.

In order to assess the perceptual influence of screen-space ambient occlusion on the perceived realism of synthetic images, three different ambient occlusion techniques of differing physical accuracy are included in the study along with a no-occlusion scenario. These four techniques are integrated into a variety of contexts varying in geometric complexity and lighting conditions, thus exhibiting different levels of ecological validity (higher visual complexity results in higher ecological validity); and are then compared to each other in different no-reference experimental scenarios. The purpose of comparing the no-occlusion scenario with an occlusion scenario is to assess whether subjects can perceive a difference, while the inter-comparison between occlusion techniques is to determine whether physical accuracy of the ambient occlusion has any bearing on perceived realism. These research goals are posited in a more formal manner in chapter 5.

The following chapter outlines previous work deemed relevant for the thesis, both in the area of screen-space visibility approximations and the area of psychophysics governing the measurements of perceptual phenomena. In chapter 3, the theory regarding ambient occlusion necessary for setting up and carrying out the ensuing experiment is covered. Chapter 4 goes into the technical details of implementing screen-space occlusion techniques in a suitable rendering framework while chapter 5 details the experimental procedure as well as presenting the results of the experiment. Chapter 6 is dedicated to the discussion and conclusion.

This page is intentionally left blank.

Chapter 2: Related Work

Previous work relevant to this thesis can be divided into two major categories. The first category is research and development of algorithms for approximating ambient occlusion in screen-space. The second category is research into the perceived realism or fidelity of synthetic images. Most relevant in the latter category is research that deals with the perception of visibility approximations such as ambient occlusion, but given that such research is sparse, key contributions on measuring perceived realism of synthetic images in general are also described. This chapter contains two sections outlining relevant work in these two categories.

Because the following section deals with screen-space approaches to computing ambient occlusion in general, previous knowledge about ambient occlusion is assumed. If the reader is unfamiliar with screen-space approaches to ambient occlusion, or just ambient occlusion in general, it is recommended to review chapter 3 first, which covers ambient occlusion from theoretical concept to practical implications.

2.1 Screen-Space Approaches to Ambient Occlusion

Several different approaches have been developed to compute dynamic ambient occlusion in screen-space. Common to all approaches is that they use a stored depth buffer (see figure 3 for two examples of a depth buffer) containing the depth of each pixel in the rendered image, to approximate scene geometry. This makes screen-space approaches' computational complexity dependent on the number of pixels in the rendered image and not the complexity of the scene geometry, a key factor which makes them a point of interest in real-time rendering. All the screen-space approaches listed in this section uses the depth buffer to retrieve an approximation of the geometry surrounding the current pixel being processed, but they differ in the way they sample this information and in the manner the ambient occlusion is calculated.

Some approaches also make use of surface normals at sampled points to further improve the results.

In the following, key screen-space ambient occlusion techniques are presented and briefly reviewed. This section constitutes a somewhat cursory look at relevant ambient occlusion techniques. A more thorough and in depth look at the theory underlying ambient occlusion is presented in chapter 3.

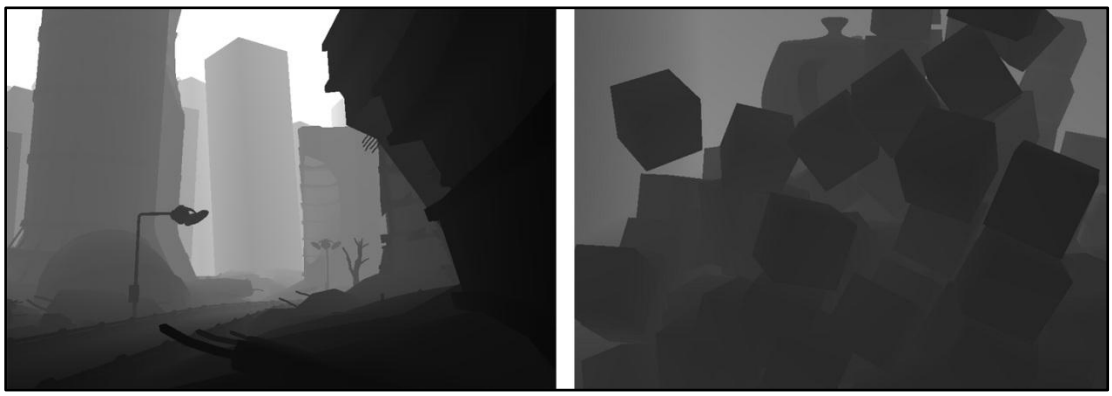

Figure 3: Two examples of a depth buffer. The depth buffer holds the depth values of all the pixels found closest to the camera. Black represents depths closest to the camera with white representing the furthest distance from the camera.

Because screen-space approaches operate on a per-pixel basis, but also samples pixels around the current pixel being processed, there can be some confusion in terminology. To aid in understanding, the term “pixel position” refers to the position of the current pixel being processed, that is, the pixel for which the ambient occlusion is being calculated. The term “sample position” and “sample point” refers to the pixels or 3D positions being sampled around the pixel position to compute the occlusion.

(Shanmugam and Arikan 2007) develop a two-pass approach that separates the computation of ambient occlusion into two parts; high frequency ambient occlusion of nearby geometry; and low frequency ambient occlusion from distant geometry. In the high-frequency pass they sample randomly distributed neighbouring samples around the pixel position in screen-space. The number of pixels sampled is controlled by the distance of the pixel position to the camera, with closer pixels receiving more

samples to provide better detail. To calculate the amount of occlusion contributed by each sample around the pixel position, a spherical *proxy* is used with an inverse square falloff to scale the occlusion with the distance of the occluding sample. The low frequency pass differs in that it uses *actual* geometry, also in the form of spheres, to compute the ambient occlusion. This pass is less flexible than the high-frequency pass as well as the other approaches mentioned in the following, in that it requires special preparation of the scene. Essentially, a second version of the scene has to be created that approximates the surface geometry of the original scene using geometric spheres. For animated scenes, the positions of the spheres are recalculated each frame based on the vertex positions of the geometry they are approximating. Figure 4 shows an example of their approach with a before and after image.

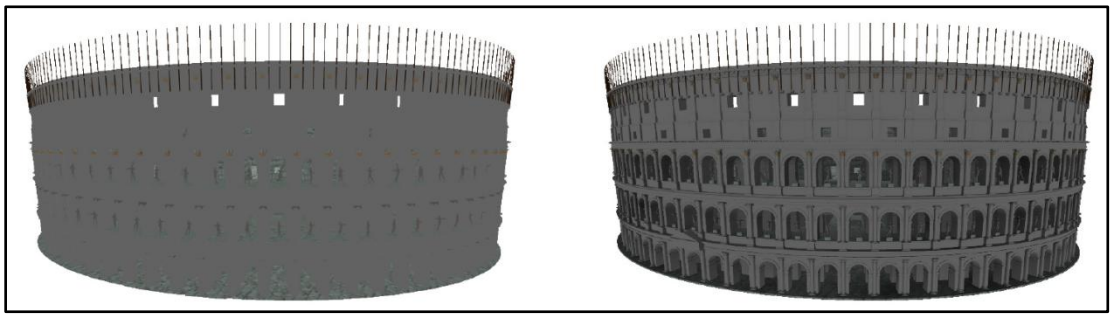

Figure 4: A before and after example of the approach by (Shanmugam and Arikan 2007). Note that this is a somewhat contrived example in that the before shot is only receiving constant ambient illumination.

(Mittring 2007) like the above mentioned approach also samples in screen space around the pixel position. However, their approach does not utilise an attenuation function, opting instead to use more samples in closer vicinity to the pixel position thus creating a stronger occlusion effect from geometry close to the pixel. A range check is implemented using a maximum value to ignore occlusion from geometry far away. The sampling process used causes distracting banding artefacts when using a low amount of samples; to offset this, the samples are randomly distributed using *jittering*, resulting in high frequency noise instead of the banding (see figure 13 on page 28 for an example). This high frequency noise is then eliminated using an edge preserving blur in a post-processing pass, taking depth discontinuities into account and only blurring samples that are close to each other in the depth buffer. See figure 5

on the left for an example of the ambient occlusion buffer resulting from this approach.

(Filion and McNaughton 2008) adopts a different approach, choosing to sample in view-space instead of screen-space. Using a predefined sampling kernel of points distributed in a unit sphere, sampling is performed in view-space around the current pixel position using 3D offset vectors. To prevent uniform banding artefacts as a result of the predefined sampling kernel and low amount of sampling points, jittering is performed by reflecting the offset vector through a random vector sampled from a texture. To improve the distribution of points and thereby the quality of the resulting ambient occlusion, a check is made whether the current offset vector is inside the hemisphere around the surface normal at the current pixel position. If the offset vector is outside the hemisphere, the vector is flipped resulting in all sample points being distributed inside the hemisphere. A post-process blur pass is also used to eliminate the noise resulting from the jittered sampling. See figure 5 on the right for an example of an ambient occlusion buffer generated using this approach.

Figure 5: On the left, an example of the ambient occlusion buffer computed using the approach by (Mittring 2007). On the right, the buffer computed using the approach by (Filion and McNaughton 2008). Please note that the left buffer is blurred while the right one is not.

(Ritschel, Grosch and Seidel 2009) compute the ambient occlusion factor in a similar fashion to (Filion and McNaughton 2008). The main contribution from their method is the addition of a directional component to the occlusion factor. All the previously mentioned approaches decouple the ambient occlusion from the illumination. In

essence, the ambient occlusion from these methods is a property of the geometry only, and is calculated without taking any light sources into account. The directional component is included by calculating the average unoccluded direction from the pixel position and using that information when calculating the illumination in a later stage. This approach can result in improved shading quality and coloured shadows when applied to direct illumination.

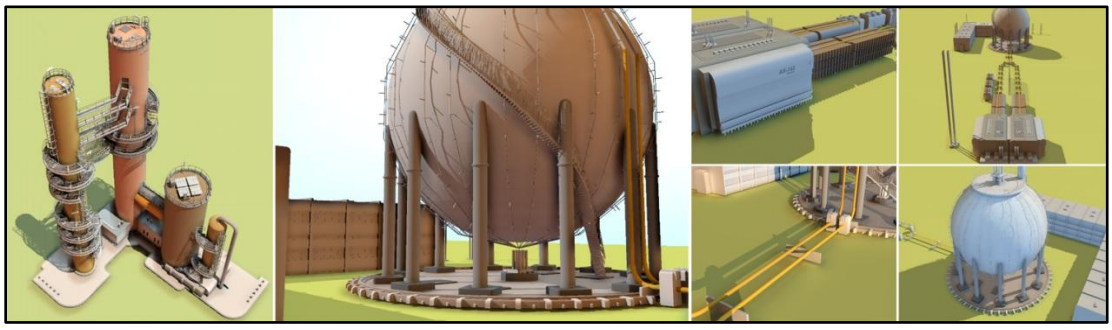

Figure 6: Some examples of the approach by (Ritschel, Grosch and Seidel 2009). Note that the strong directional shadows in these images are from shadow mapping and not ambient occlusion.

In this section some key approaches to calculating ambient occlusion in screen-space were reviewed. In chapter 3, the underlying theory of ambient occlusion is covered in more detail.

2.2 Measuring Perceived Realism of Synthetic Images

In this section, related work on measuring perceived realism or rendering fidelity is presented and reviewed. The material covered in this section is expanded upon in chapter 5 dealing with the design and execution of the experimental procedure.

A closely related study to this thesis is presented by (Yu, et al. 2009). Their work details a psychophysical study into the perceptual effect of approximating visibility in indirect illumination. While this might sound close to identical to the present study, their contribution does differ significantly in that it uses experimental stimuli created using offline rendering methods. More specifically, a radiosity solution is used to render the scenes using four bounces of indirect illumination; and different visibility

approximations, including ambient occlusion, are then used to attenuate the indirect illumination. The stimuli consist of four different scenes rendered out in five second video sequences at a resolution of 640 by 480 pixels, with between one and four hours of rendering time dedicated to each frame of the animation. This of course makes the context of their experiment radically different, even though they are investigating a similar research question.

Two different experiments were performed. The first is a two-alternative forced choice scenario used to quantify the perceptual similarity of the different visibility approximations to a ground-truth reference using accurate visibility determination. The second is an *ordinal rank order* method used to gauge the perceived realism of the different approximations in relation to each other. In this experiment, subjects were allowed to compare all different approximation directly and were then asked to assign a relative rating to each. The outcome of these two experiments are quite interesting and show that visibility approximations can produce results that are perceptually similar to reference renderings using physically accurate visibility.

(Sundstedt, et al. 2007) also conducts a psychophysical study into the perceived quality of synthetic images. In this case the subject of scrutiny is the rendering of participating media, to which they present their own novel approach. It is of course the perceptual experiment that is of interest here and not the rendering algorithm used. Similar to the previously cited study, this contribution also deals with an offline rendering scenario but does exhibit the distinction of carrying out a no-reference study in addition to a traditional reference procedure. In the no-reference scenario, an approximation was compared to a gold standard reference without allowing any direct comparison between the images. To facilitate this indirect comparison, the two images were presented for four seconds each, with a two second medium-grey image in between. The procedure here was a two-alternative forced choice, same as the first experiment presented in the previous paragraph.

(Jimenez, Sundstedt and Gutierrez 2009) adopts the experimental no-reference approach presented in the previous paragraph, but in a real-time rendering context.

One pertinent difference is that instead of using fixed timing intervals between the showing of each image, they allow the subject to control the time taken to study each image themselves, but encouraging them to spend about ten seconds on each image. The specific context of their experiment is screen-space rendering of human skin, and their results suggests that the no-reference experimental approach can provide useful perceptual measurements.

Finally, (Kozlowski and Kautz 2007) presents both a reference and no-reference scenario within the context of rendering glossy reflections in real-time. The reference scenario here is similar to the *ordinal rank order* method presented in (Yu, et al. 2009) while the no-reference scenario differs from the approaches mentioned so far. Here, experiment participants were presented with a random order of sixty images, with a blank image displayed between each, for half a second, to prevent any direct comparison. Instead of a forced choice alternative, subjects were asked to rate the presented images from high to low, on two different scales; the first scale was defined as realism with regards to lighting, shadowing and reflections, while the second was defined in aesthetic terms, simply asking the subject to rate the image according to how pleasing it was in appearance.

Their results are of particular interest to this study and also highlight the inherent problem of using a reference experiment condition to evaluate perceived realism, making the following observations in their paper; when given no reference for comparison, different kinds of approximations (in their case related to the occlusion of glossy reflections) can result in perceptually realistic results. However, given the opportunity for direct comparison (the reference condition), all the approximations tested in their study became identifiable as such and the more accurate ground truth image was chosen as the most realistic. Of equal interest were their findings that the complexity of the scene had a significant effect on the perceived realism of the different approximations used. In general, when using more complex (and consequently more ecologically valid) scenes, the approximations used are perceived as exhibiting higher visual realism than in cases where simpler scenes are used. More

concisely, the approximations hold up in complex scenarios but fail in simpler, more contrived scenarios.

This section served to highlight and review previous work and studies that are relevant to the thesis. In the following chapter, the necessary theory regarding ambient occlusion is covered in depth to facilitate the implementation of the screen-space techniques that are investigated in the experimental study.

Chapter 3: Theory

In this chapter, the theory underlying the different approaches to calculating ambient occlusion is presented and reviewed. While the area of interest for this thesis is that of techniques performed in *screen-space*, it is more useful to first look at ambient occlusion from a more *object-space* oriented perspective. The reason for this is that object-space approaches present a more comprehensible analogy to the real world than screen-space approaches, and it is easier to consider approaches in screen-space with a solid understanding of how the process works in object-space.

The chapter is split into several sections. First, the conceptual and mathematical background for ambient occlusion is covered. Following that, the presented theory is carried over to the practical, presenting a typical ray-traced approach to calculating ambient occlusion in object space. Finally, the general process of computing ambient occlusion in screen-space is presented. The last section is intended to highlight key differences in moving from object-space to screen-space, preparing for the following chapter in which the implementation of different screen-space techniques are described.

3.1 A Conceptual View of Ambient Occlusion

Before discussing ambient occlusion it is important to consider the specific lighting phenomena it affects. As briefly touched upon in the introduction, ambient occlusion is a term that is used to modulate the amount of indirect (ambient) light a shaded point in the scene is receiving. In its simplest form, ambient light is just a constant factor that does not vary with direction and has a constant value termed L_A. In geometric terms, it represents the amount of illumination coming from all possible directions (the *irradiance*) contained within the hemisphere that is oriented around the surface normal of the currently shaded point. Figure 7 illustrates both direct and indirect illumination geometrically. A common approach in real-time rendering

scenarios is to simply set the ambient light contribution to the diffuse colour of the point being shaded and then scale by the ambient light amount represented by L_A (Möller, Haines and Hoffman 2008, 296).

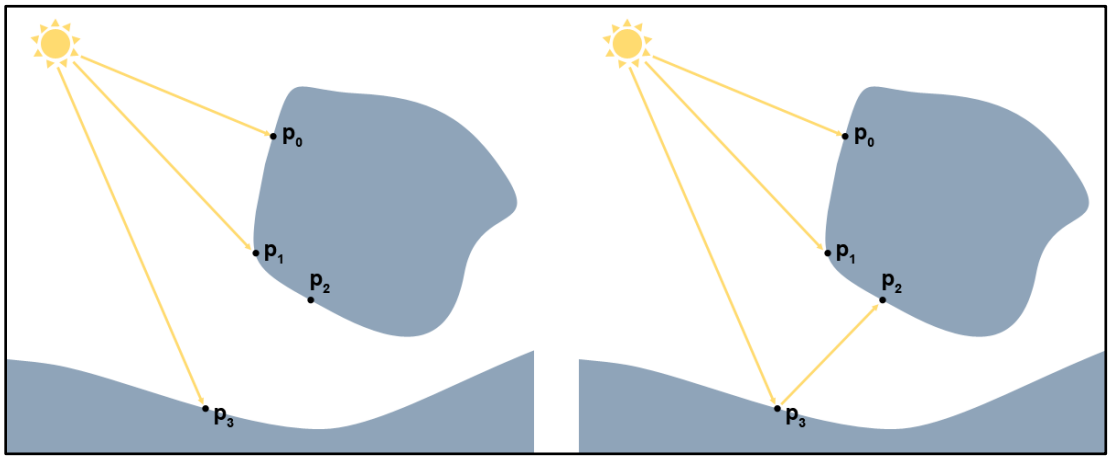

Figure 7: A simplified illustration of the difference between local and global illumination. On the left, the point P_2 is not receiving any illumination because the light source cannot "see" it. On the right, P_2 is receiving indirect bounced illumination from the surface at P_3. Calculating such bounces is not feasible in real-time rendering, so approximations are often used.

This approach provides a marked improvement in rendering quality over using direct illumination only, since surfaces that are in shadow or facing away from the light would otherwise be completely black (see figure 8). Regardless, the effect of using a constant ambient illumination model is flawed and ultimately provides unsatisfying results due to its simplified nature. Two main reasons contribute to this. First the model does not take into account that indirect light coming from the environment is *not* constant and that it varies both in colour and intensity depending on the surrounding geometry of the environment. More specifically, a portion of the illumination from a light source striking a surface will be reflected and illuminate other nearby surfaces. This bounced light will retain some colour from the surface it was reflected from and thus carry this coloured light to other surfaces in a process known as colour bleeding (Möller, Haines and Hoffman 2008, 408).

The second reason is that the model does not take occlusion into account when computing the amount of indirect light a surface point is receiving. Surrounding geometry will block some of the incoming light from the environment causing a

darkening in the form of soft shadows where there is a lot of surrounding geometry. A physical approach to modelling this occlusion effect would be to calculate accurate visibility for all bounces of indirect light. Obviously, this is simply not practical for real-time purposes and is often forgone in offline rendering scenarios as well when rendering time is a factor.

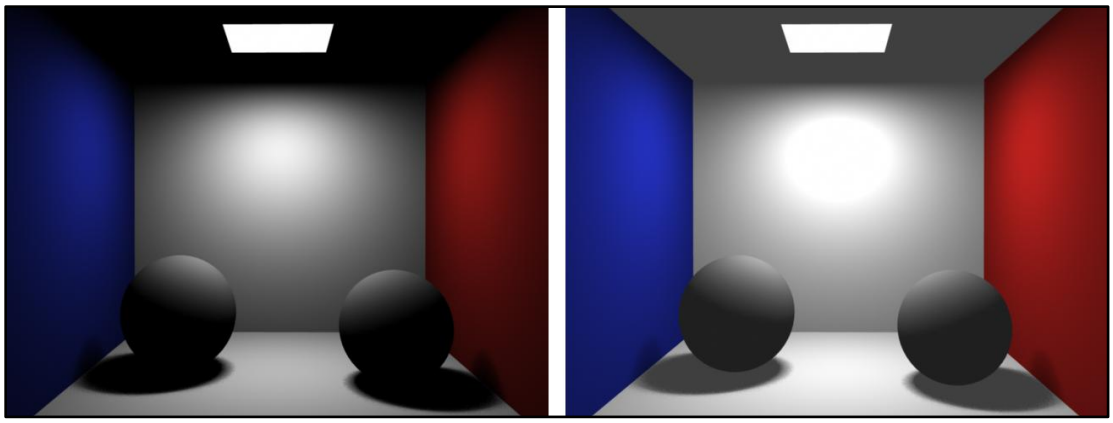

Figure 8: The effect of constant ambient light. On the left, the Cornell box is rendered using local illumination only. On the right, all surfaces are receiving 25% of their diffuse color as ambient light.

Ambient occlusion is an approximation of the physical approach used to accurately simulate visibility in indirect illumination. Instead of computing correct visibility, the approach is instead to calculate an ambient occlusion *coefficient* determined by the amount of surrounding geometry, and then modulate the ambient light contribution by this coefficient. How the coefficient is calculated differs between implementations and is covered in more detail in the following sections. Ambient occlusion is essentially an empirical model that is based on the perceptual observation that occluding geometry will result in soft shadowing. Consequently, ambient occlusion can naturally be considered shadowing of ambient light (Möller, Haines and Hoffman 2008, 374).

In summary, constant ambient lighting can improve rendering by preventing surfaces that are in shadow or facing away from light sources from appearing pitch black (as in figure 8 on the left). However, using constant ambient lighting causes objects to appear flat because light is incoming evenly from all directions. Ambient occlusion addresses this problem by modelling soft shadowing from surrounding geometry.

Figure 9 illustrates constant ambient lighting with and without ambient occlusion applied (actually, the constant ambient light seen in figure 9 is just the colour of the texture, which is equivalent to an ambient light intensity of 1).

Figure 9: The Stanford dragon model rendered using constant ambient lighting alone, and constant ambient lighting with ambient occlusion applied.

3.2 A Mathematical View of Ambient Occlusion

In this section a more detailed view of ambient occlusion is presented. In the previous section, constant ambient light was mentioned as the simplest form of indirect illumination. For the sake of simplicity, only Lambertian diffuse surfaces are considered in the following, but the equations presented here can be extended to cover arbitrary bidirectional reflectance distribution functions *(BRDFs)* (Möller, Haines and Hoffman 2008, 223). With that in mind, the constant ambient light L_A results in a constant amount of outgoing illumination that does not take the surface normal or view direction into account. This ambient light can be expressed in the context of irradiance in the following equation:

$$E(\mathbf{p}, \mathbf{n}) = \int_{\Omega} L_A \cos\theta_i d\omega_i = \pi L_A \quad (1)$$

Here, E represents irradiance for the point $\mathbf{p}$ with surface normal $\mathbf{n}$, which is the cosine weighted integral of incoming radiance performed over the hemisphere Ω for all possible incoming directions (Möller, Haines and Hoffman 2008, 374). As mentioned, this model does not take visibility or surface orientation into account which results in the flat appearance seen in figure 9. Extending this equation to include a simple visibility (occlusion) function $v(\mathbf{p}, \mathbf{l})$ first presented by (Cook and Torrance 1981) results in the following equation:

$$E(\mathbf{p}, \mathbf{n}) = L_A \int_{\Omega} v(\mathbf{p}, \mathbf{l}) \cos\theta_i d\omega_i \tag{2}$$

The visibility function can vary in complexity. In its simplest form the function returns a binary value; 0 if the ray representing the incoming direction $\mathbf{l}$ to the point $\mathbf{p}$ is blocked, and 1 if it is not. As mentioned in the previous section, the ambient occlusion is actually a coefficient used to modulate the incoming irradiance. This coefficient is termed $k_A$and to calculate it, the following equation is derived from (2):

$$k_A(\mathbf{p}) = \frac{1}{\pi} \int_{\Omega} v(\mathbf{p}, \mathbf{l}) \cos\theta_i d\omega_i \tag{3}$$

The value of the coefficient k_A lies in the range of 0 to 1. If the value is 0, the point $\mathbf{p}$ is completely occluded and is receiving no ambient light. If the value is 1, the point is receiving full irradiance which is equivalent to equation (1). Figure 10 illustrates ambient occlusion geometrically. The black arrows represent the occluded directions while the yellow arrows represent the unoccluded directions. The brightness of the yellow arrows illustrates the effect of the cosine factor present in equation (2) and (3). The visibility function $v(\mathbf{p}, \mathbf{l})$ is weighted by this cosine factor when integrated, which changes the visibility from a simple binary function to a ranged one. This has the effect of taking the surface orientation into account when calculating the ambient occlusion coefficient k_A (Möller, Haines and Hoffman 2008, 375). As a result, $\mathbf{p}_0$ is receiving more irradiance than $\mathbf{p}_1$ because the incoming light is centred around the surface normal, even though their average unoccluded solid angle is similar in size.

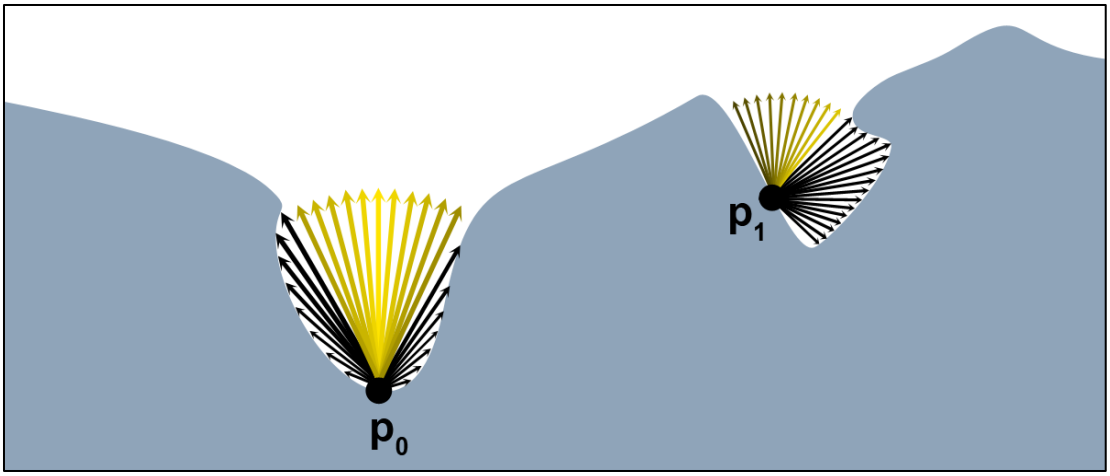

Figure 10: Illustrates Ambient Occlusion at points p_0 and p_1. The black arrows represent occluded directions while the yellow arrows represent unoccluded directions. The brightness of the unoccluded directions illustrates the cosine factor used as a weight when calculating the occlusion coefficient k_A.

Once the ambient occlusion coefficient has been calculated it is a simple matter to calculate the amount of irradiance the shaded point is receiving using the following equation:

$$E(\mathbf{p}, \mathbf{n}) = k_A(\mathbf{p})\pi L_A \tag{4}$$

Equation (4) is just the ambient occlusion coefficient calculated for the point **p** multiplied with the incoming ambient illumination given in equation (1).

3.3 Shading with Ambient Occlusion

Applying equation (3) in a practical context is not always a workable solution. When calculating ambient occlusion for a discrete object such as a character model, the equation can be applied directly and either be pre-computed in an offline render pass or be computed dynamically. However, this does not take into account the occlusion of other nearby geometry in a scene. In the case of a character, when the model is integrated into a scene and e.g. appears in the close vicinity of other geometric

objects, these objects are not contributing occlusion to the character model and vice versa.

Moreover, the approach breaks down entirely when applied to a situation of enclosed geometry such as a room. When evaluating the visibility function $v(\mathbf{p}, \mathbf{l})$ in practice, the light ray **l** is checked for intersection with the geometry of the scene to determine if the incoming light is blocked. In the case of an enclosed space, the visibility function will always evaluate to zero because the light ray always intersects some geometry, which has the effect of all points being shaded completely black (assuming that the point is only receiving ambient illumination). To address this issue, the visibility function $v(\mathbf{p}, \mathbf{l})$ is usually replaced with a distance mapping function $\rho(\mathbf{p}, \mathbf{l})$. This approach called *obscurance*, first presented by (Zhukov and Iones 1998), changes the visibility from a binary function to a continuous function of the distance to the intersection. A user specified maximum distance d_{max} is used to limit the range in which intersection is tested for. The distance function then returns a value of 0 for intersection distances of 0, and 1 at intersection distances of d_{max}. Distances beyond d_{max} are not checked, solving the issue of enclosed geometry in addition to decreasing the computational cost of computing k_A considerably.

Shading with ambient occlusion is best explained using the full shading equation (Möller, Haines and Hoffman 2008, 376) which also takes direct illumination into account:

$$L_o(\mathbf{v}) = k_A \frac{\boldsymbol{c}_{amb}}{\pi} \otimes \pi L_A + \sum_{k=1}^{n} v(\mathbf{l}_k) f(\mathbf{l}_k, \mathbf{v}) \otimes E_{L_k} \overline{\cos}\theta_{i_k} \quad (5)$$

The term L_o computed here is the outgoing radiance along the view direction **v** and is invoked for each pixel in the rendered image. Because the shading equation works with coloured lights, which are treated as RGB vectors in practice, the symbol $\otimes$ is used to denote per-component vector multiplication. The term on the left of the addition sign is the ambient light using ambient occlusion, while the term on the right side is the direct illumination from k light sources. For the direct illumination;

$v(\mathbf{l}_k)$ is the visibility function which can be evaluated using e.g. shadow mapping; $f(\mathbf{l}_k, \mathbf{v})$ is the bi-directional reflectance distribution function; E_{L_k} is incoming radiance from light source k; and the last term is the clamped cosine factor of the angle between the incoming light direction and the surface normal. The factor is clamped between 0 and 1 to avoid backlighting of surfaces.

Of course, it is the ambient term that is of interest here, and only the term $\boldsymbol{c}_{amb}/\pi$ remains unexplained. The $1/\pi$ factor is present because the result of integrating a cosine factor over the hemisphere gives a value of π (Möller, Haines and Hoffman 2008, 228). In real-time rendering scenarios, this is usually rolled into the value of $\boldsymbol{c}_{amb}$ for practical purposes. The value of $\boldsymbol{c}_{amb}$ for Lambertian surfaces is simply the diffuse colour of the surface. For non-Lambertian surfaces, the value is a blend of the diffuse and specular colours. Figure 11 shows four different rendering scenarios applying different elements of the full shading equation presented in (5).

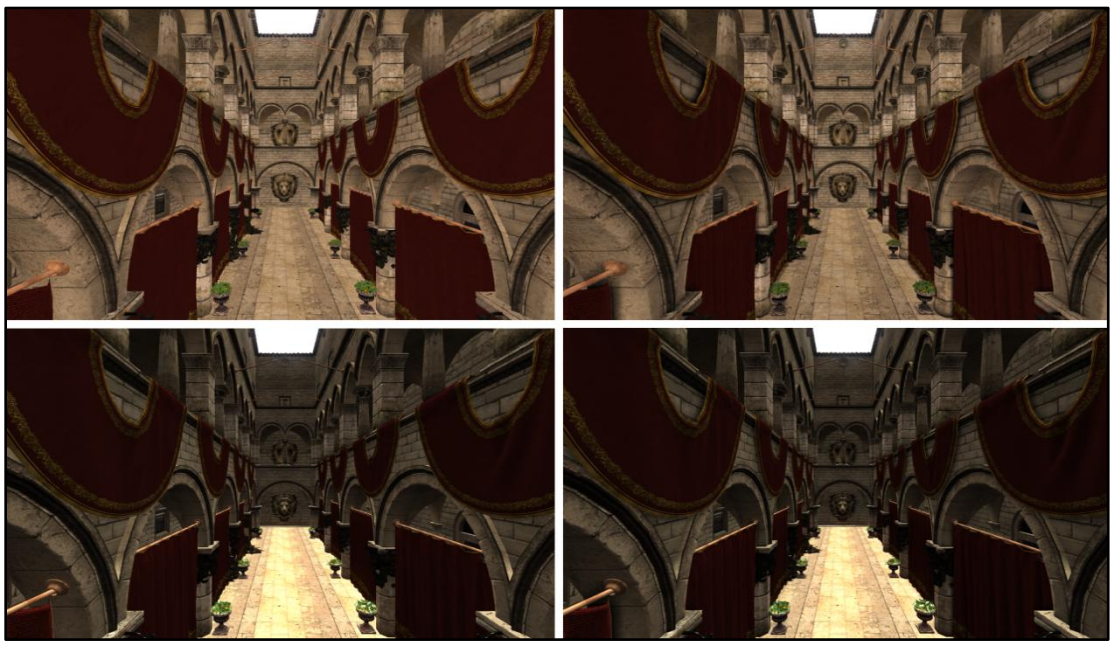

Figure 11: Top left: Ambient light only. Top right: Ambient light with ambient occlusion. Bottom left: Ambient and one directional light. Bottom right: Ambient and one directional light with ambient occlusion.

As is evident from figure 11, the effect of ambient occlusion is less pronounced when direct illumination is included. This can be offset by applying k_A to directional lights

as well, although this is incorrect and will result in darkening of areas where any direct illumination would prevent such a darkening.

The following two sections take a more pragmatic approach to ambient occlusion than the mathematical one presented in this section.

3.4 Ambient Occlusion in Object-Space

Calculating ambient occlusion in object-space has in large part already been covered in the previous section. However, the coverage in the previous section was very theoretical and the content here serves to provide a more accessible example on how to calculate ambient occlusion in object space. The material in the previous section applies both to the scenario of pre-computing ambient occlusion as well as the scenario of computing it dynamically. From this point on, only dynamic computation of ambient occlusion is considered.

Because the integral in equation (3) is prohibitively expensive to calculate, a different approach is usually taken to perform sampling within the hemisphere. A common approach is to use a Monte Carlo method to generate a uniform distribution of sampling directions in the hemisphere oriented around the surface normal. Each generated direction is then treated as a ray for the purpose of testing for intersections with scene geometry. For complex scenes, this is still computationally expensive, and a pre-computed acceleration structure is usually employed to prevent intersection tests with all triangles in the scene. The reason the introduction of the distance function presented in section 3.3 reduces the computational cost should be evident in that it further reduces the amount of geometry to perform intersection tests on.

The approach presented in the previous paragraph is a common one for offline rendering scenarios, but is only useful in real-time rendering for the purpose of pre-computing static ambient occlusion in a scene. To leverage fully dynamic ambient

occlusion in a real-time rendering context, the process has to be moved into screen-space.

3.5 Ambient Occlusion in Screen-Space

The primary reason the object-space approach presented in section 3.4 is unsuitable for real-time purposes, is its dependency on the complexity of the scene being rendered, more specifically the amount of polygons present in the scene. For contemporary real-time rendering scenarios such as computer games, scene complexity has long since passed the point where an object-space approach would be feasible for dynamic computation.

Screen-Space approaches to calculating ambient occlusion are not dependent on the scene complexity since they are performed in a post-processing pass on the rendered image. However, screen-space approaches are still based on the same conceptual basis presented in section 3.1 and therefore still need to access some form of the scene structure to compute the occlusion factor k_A. This scene structure is present in the form of the depth-buffer (Z-buffer) of the rendered scene, which contains the depth of all the pixels that have passed the depth test (i.e. all the visible pixels). In general terms, screen-space approaches use the information in the Z-buffer as a limited representation of the full scene geometry to perform the sampling used for calculating the occlusion factor. In other words, the distance function in section 3.3 is not performed on the actual scene structure using intersection testing, but rather as a 2D sampling process that relies on the inherent properties of the stored depth-buffer.

Figure 12 shows a typical example of how the depth buffer can be utilized as a limited scene structure for performing screen-space ambient occlusion. A certain amount of points are sampled in the sphere around the shaded point **p**. The depth of each sample point is compared to the depth found at the sample pixel in the depth buffer. If the depth of the sample point is greater than the depth stored in the buffer, the sample is considered inside the geometry and is categorized as an occluder.

Samples with depth values less than the depths stored in the buffer are categorized as non-occluders and the ambient occlusion term k_A is computed as the ratio between occluders and non-occluders using the difference in depth between samples as a weight (Möller, Haines and Hoffman 2008, 383).

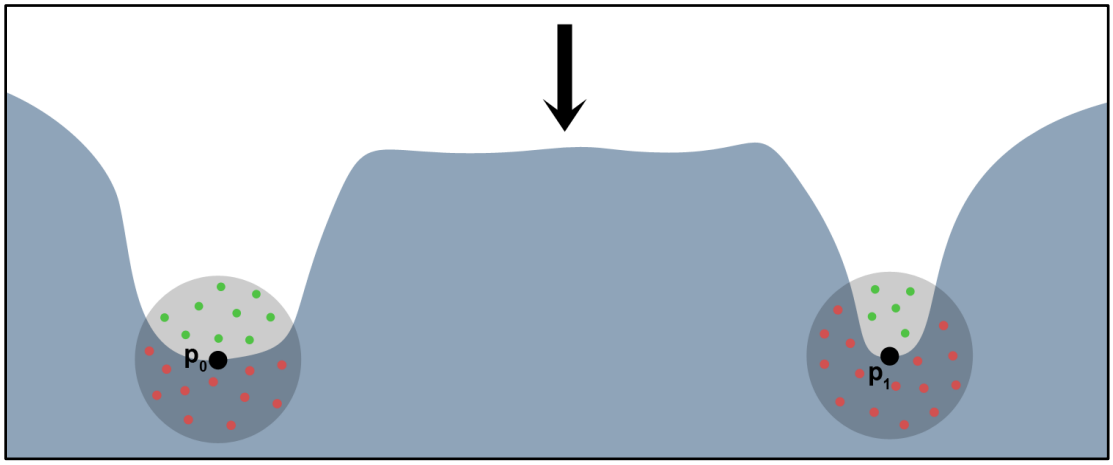

Figure 12: Illustrates a common approach to screen-space ambient occlusion. Green sample points are considered non-occluders while the red sample points are considered occluders. The ambient occlusion is calculated as the ratio between occluders and non-occluders. The illustration is shown in 2D for clarity with the black arrow representing the viewing direction of the camera. The radius of the sampling spheres is determined by the parameter d_{max} introduced in section 3.3.

Certain issues arise from this approach. Since the only information available is the visible pixels, occlusion from non-visible surfaces is not taken into account. The same holds for geometry that is off-screen. Furthermore, it requires many samples to generate good visual quality which is not feasible on current generation hardware. Using a low amount of samples results in a distracting and undesirable banding pattern illustrated on the left in figure 13. To counteract this, the process of jittered sampling is used where a different sampling pattern is used for each 4x4 pixel block. This converts the banding artefacts into high frequency noise shown on the right in figure 13. This noise is then dealt with in a subsequent rendering pass using a bi-lateral blur filter that does not blur across depth discontinuities (Möller, Haines and Hoffman 2008, 383).

The two images in figure 13 holds the value of the ambient occlusion coefficient k_A for each pixel. Intuitively, multiplying such a grey-scale image with a

colour buffer holding the rendered scene, which is what equation (4) and (5) does, will result in a darkening in the areas where the occlusion buffer is darker.

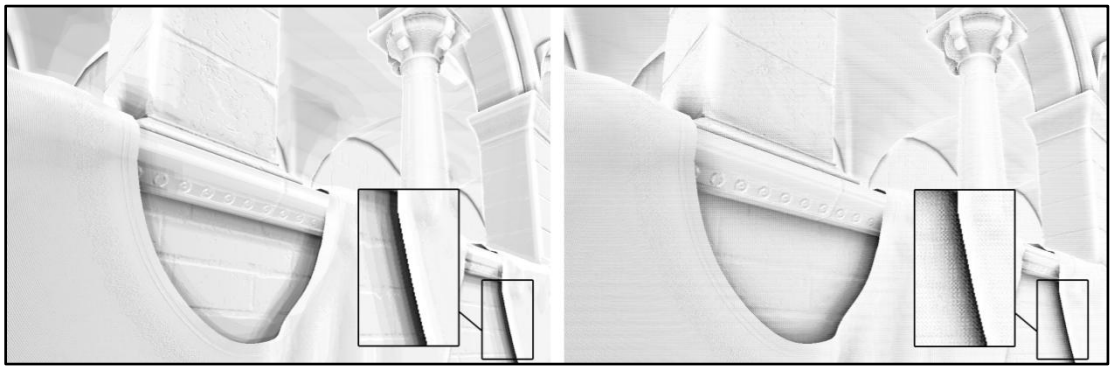

Figure 13: Illustrates the use of jittered sampling to convert banding artefacts into high-frequency noise. On the left the banding is very evident on the arched roof and the heavily occluded areas near the cloth banner. On the right, these artefacts have been turned into high frequency noise by the jittering process. When the buffer is blurred, the banding is noticeable while the noise is not.

3.6 Chapter Conclusion

In this chapter, a conceptual, theoretical and practical overview of ambient occlusion was presented. There are many different ways to approach ambient occlusion in both object-space and screen-space and only a few were highlighted here. However, the contents were carefully reviewed in order to ensure that the necessary areas were covered, forming the required knowledge necessary for the following chapter on the practical implementation of ambient occlusion in screen-space.

Chapter 4: Implementation

This chapter deals with the implementation of ambient occlusion in screen-space necessary for setting up the experiment outlined in chapter 5. The chapter is split into several different sections dealing with the choice of what occlusion techniques to implement; the process of implementing a suitable rendering framework into which the chosen ambient occlusion techniques can be integrated; the actual implementation of the chosen techniques; and in the last section, some additional implementation considerations regarding the implementation process as a whole and the ensuing experiment.

Even though a considerable amount of code was written in implementing the framework outlined in section 4.2, said section maintains a conceptual style forgoing any code samples. Conversely, section 4.3 describing the implementation of the ambient occlusion techniques presents plenty of code samples to illustrate the process. The presented code is written in Microsoft's high level shading language (HLSL) and prior experience with either this language; the OpenGL shading language (GLSL); NVidia's C for graphics (CG); or even regular C is recommended to get a comprehensive understanding of the contents.

4.1 Choice of Ambient Occlusion Techniques

The choices regarding which screen-space ambient occlusion techniques to implement are of course determined by the research question posed and the nature of the study. Two primary goals for the experimental study were outlined in section 1.2; the first, to investigate the effect of ambient occlusion on perceived realism; the second, to assess the effect that physical accuracy of a given technique has on perceived realism. With these two goals in mind at least two ambient occlusion techniques that differ in physical accuracy are needed.

To cover this need, the two techniques chosen were by (Mittring 2007), described in section 4.3.1, and by (Filion and McNaughton 2008), described in section 4.3.2; both were briefly covered in section 2.1. The two were chosen because of a significant difference in accuracy and apparent quality; although whether this quality difference is perceivable by naïve (with regards to the experiment purpose and background) human observers of course remain to be seen.

In addition to these two techniques, a third modified version of the second technique was also implemented. This technique is more accurate and is described in section 4.3.3. While not strictly needed to address the research question, it was included to create an experiment condition with a large disparity in algorithm accuracy. For more details on this, see section 5.3 describing the creation of the experiment stimuli.

4.2 Implementing a Suitable Rendering Framework

The two deciding factors in implementing the rendering framework were development speed and image quality. The development speed requirement precluded the use of the more powerful rendering APIs such as DirectX and OpenGL, since they require a substantial amount of work to get a full rendering context up and running. A good compromise between development speed and quality was found in Microsoft's game development suite XNA. It provides extensive functionality out of the package and it is easy and relatively quick to get a rudimentary rendering context running. Beyond that, XNA provides excellent support for using custom shaders making it a suitable choice for setting up a rendering framework.

As mentioned, no code is shown in this section but the entirety of the code written can be found on the accompanying CD. The remainder of this section serves as a conceptual overview of the rendering framework implemented allowing for the integration of the different ambient occlusion techniques to follow.

In section 2.1 it was established that screen-space ambient occlusion techniques requires a depth buffer for sampling the scene structure and that some approaches require the surface normals of shaded pixels as well. Regarding the techniques described in this chapter, the first only uses the depth information while the last two use the surface normals as well. The basic requirement of having access to both scene depth and surface normals had a significant bearing on the manner in which the rendering framework was implemented.

Because screen-space ambient occlusion techniques (and screen-space techniques in general) are carried out in a post-processing pass, i.e. they are performed after the scene has already been rendered; accessing the scene depth and especially the surface normal is not a trivial matter. An additional issue is presented due to the way the underlying graphics API (in this case DirectX) stores the depth of the rendered pixels. The depth is stored in a non-linear depth buffer with more precision allocated to scene elements that are closer to the camera. This works well for sorting objects which is the primary purpose of the depth buffer, but this non-linearity is not ideal for techniques such as ambient occlusion. This creates the additional requirement of having access to a linear version of the depth buffer with equal precision across the entire range of the scene.

Following the considerations in the previous paragraph, screen-space techniques lend themselves well to a deferred rendering framework (sometimes referred to as deferred shading). Deferred rendering or shading means that the scene is rendered to several different render targets called Geometry Buffers (G-buffers, see figure 14 for an example), which are just 2D textures, and lighting is then deferred to a later stage of the rendering, performed as a 2D post-process similar to screen-space techniques such as ambient occlusion. The common reason for using deferred rendering is that the approach can handle a large amount of dynamic lights; however, this is not what makes it of interest in this context. Common data rendered to the G-buffer in a deferred rendering context includes scene depth and surface normals, which means

that in a deferred rendering context, this data is readily available for all post-processing operations including screen-space ambient occlusion.

For these reasons, a deferred rendering framework was implemented in XNA which could easily support several different screen-space ambient occlusion techniques. Figure 14 shows the basic flow of the deferred rendering framework. A few details such as ambient lighting and high-dynamic range processing have been left out of the figure for the sake of clarity.

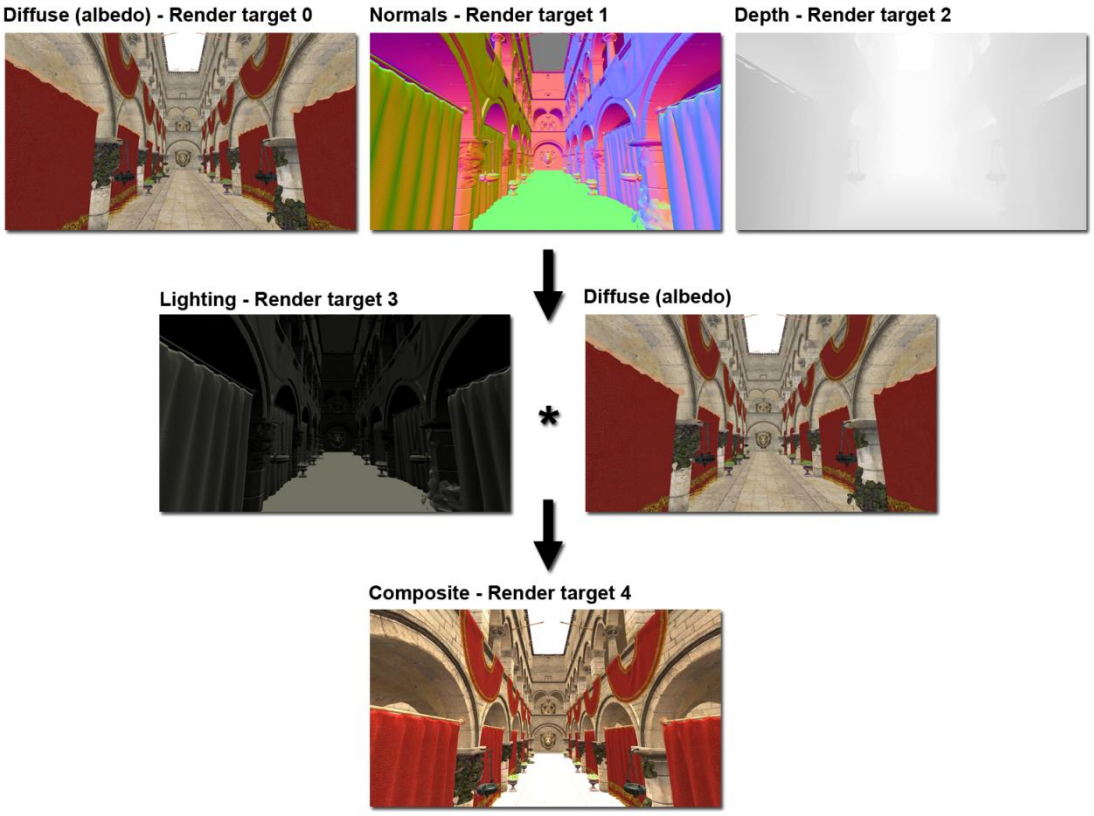

Figure 14: Illustrates the rendering flow of the deferred rendering framework. The G-buffers are rendered first and consists of the diffuse colour, surface normals, and scene depth. Lighting is then performed using the stored normals and depth. Modulating the diffuse colours with the lighting creates the composite image shown at the bottom.

The important point to illustrate here is that once the final colour image is rendered (shown on the bottom), the diffuse, normal and depth information is retained and is free to be utilised in a post-processing pass, be it colour grading, depth of field, ambient occlusion, or some other post-processing technique.

The format of the 2D render targets holding the stored information of the G-buffers is important, and should be carefully chosen for the desired output. Most importantly, the depth buffer needs at least 16 bits to properly represent the depth of the scene. Using lower bit depths results in banding artefacts in the lighting and more importantly, unusable ambient occlusion results due to insufficient precision. Table 1 illustrates the render targets used for the basic deferred rendering setup.

Table 1: The three render targets used for the basic deferred rendering setup. Two four channel 32 bit targets were used for the diffuse, specular and normal data. A single channel 32 bit render target was used to store the linear depth.

Target / Channel	Red	Green	Blue	Alpha
Render target 0 8 bits/channel	Red Diffuse	Green Diffuse	Blue Diffuse	Specular Intensity
Render target 1 8 bits/channel	Normal X	Normal Y	Normal Z	Specular Power
Render target 2 Single Channel	Depth (32 bits)			

A few additional render targets were used in addition to these fundamental ones. The most important ones are listed in table 2.

Table 2: Additional render targets used: Render targets 3 and 4 uses 16 bits per channel to enable high dynamic range lighting. Only one 8 bit channel is needed for the ambient occlusion coefficient.

Target / Channel	Red	Green	Blue	Alpha
Render target 3 16 bits/channel	Red Light	Green Light	Blue Light	Specular Light (monochromatic)
Render target 4 16 bits/channel	Red Final Colour	Green Final Colour	Blue Final Colour	Unused
Render target 5 8 bits / channel	Unused	Unused	Unused	Ambient Occlusion Coefficient

Extending the basic setup shown in figure 14, figure 15 shows the remainder of the deferred rendering process. Again, for the sake of clarity some steps are left out such as the blur pass of the ambient occlusion buffer.

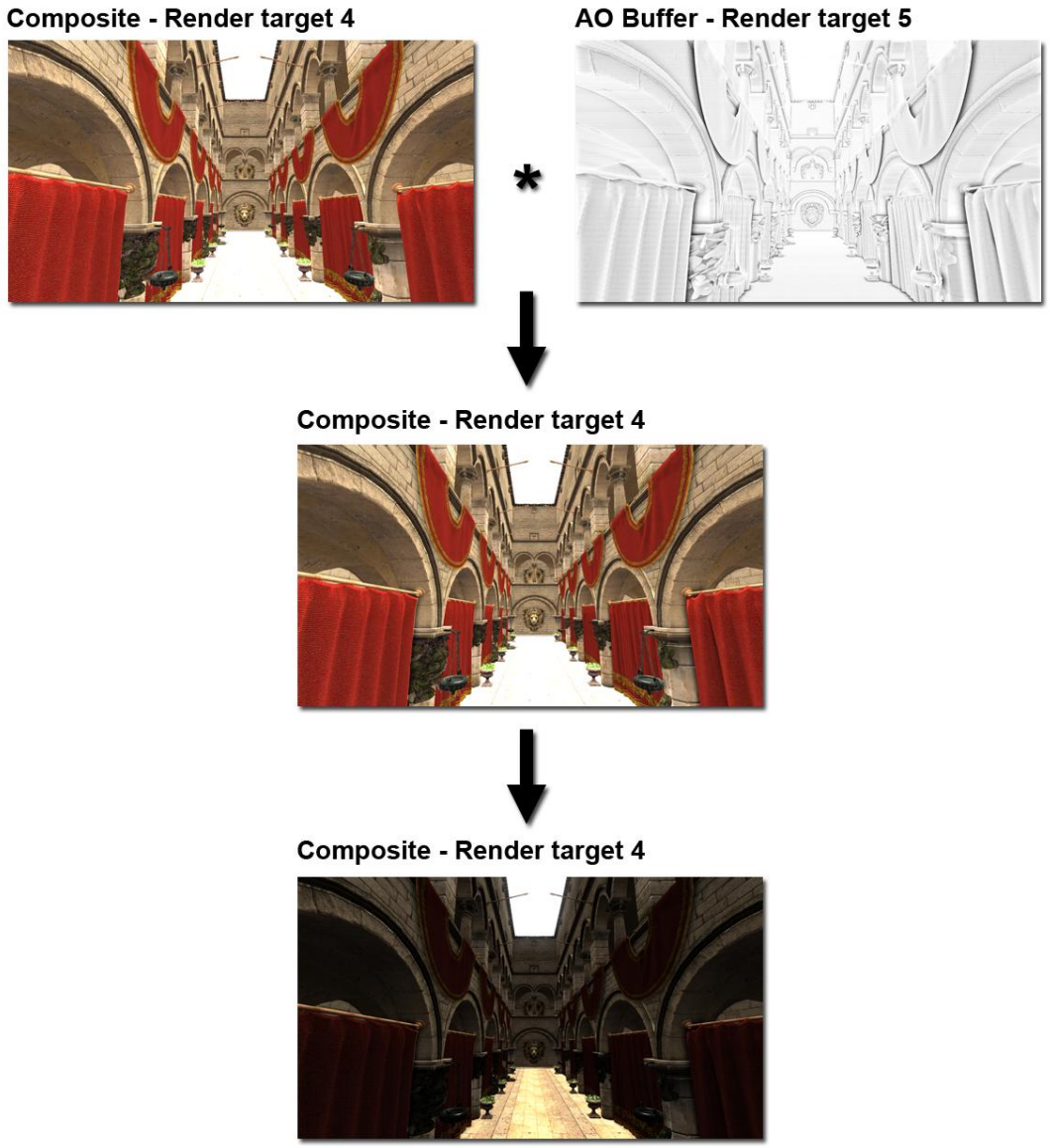

Figure 15: The final steps of the deferred rendering process. The last operation resulting in the final image is a tone mapping operator, mapping the high dynamic range values to be displayed on a low dynamic range device. When not using high dynamic range lighting, very bright areas are clipped to white as seen in the middle image. Note how render target 4 is reused several times. The multiplication of the ambient occlusion buffer is actually taking place in the compositing step of figure 14 while the tone mapping is operating on a copy of render target 4. Sampling from, and writing to, the same render target in one pass is not allowed.

The choice of implementing the rendering framework in the manner presented here allowed for easy integration of multiple screen-space ambient occlusion techniques. The following section outlines the implementation of the three techniques used in the experimental study.

4.3 Implementing the Ambient Occlusion Techniques

For the sake of brevity, the different techniques described here have been given specific names. For the first two techniques, the names given are that of the respective companies from which the techniques originated, Crytek (Mittring 2007) and Blizzard (Filion and McNaughton 2008). The third technique is an extension of the Blizzard technique and is named Ray-Marching, the reasons for which are outlined in section 4.3.3.

Code comments are not included here since the comments are usually covered in the text, but all three ambient occlusion shaders can be viewed in full, including comments, in the appendix or on the accompanying CD.

The contents of the following three sections can be difficult to follow and the following conventions should aid in understanding. Each ambient occlusion technique is performed in a full-screen post-processing pass, which is essentially a large loop iterating through each pixel of the image being processed. When performing ambient occlusion, the image being processed is of course the stored depth buffer. For each pixel, another loop structure is utilised to generate samples around this pixel used in accumulating the ambient occlusion. An important point to remember is that each pixel in the depth buffer represents the world space position of the surface point that was found closest to the camera. Any samples generated around this point also represent positions in world space. However, the positions of these samples also correspond to positions stored in the depth buffer, but the position in the depth buffer will usually have a different depth than the sample position. Computing the difference between the depth of the sample pixel and the depth of the pixel position, we can figure out if the current sample position is in front or behind the point stored in the depth buffer. Figure 16 illustrates the process visually.

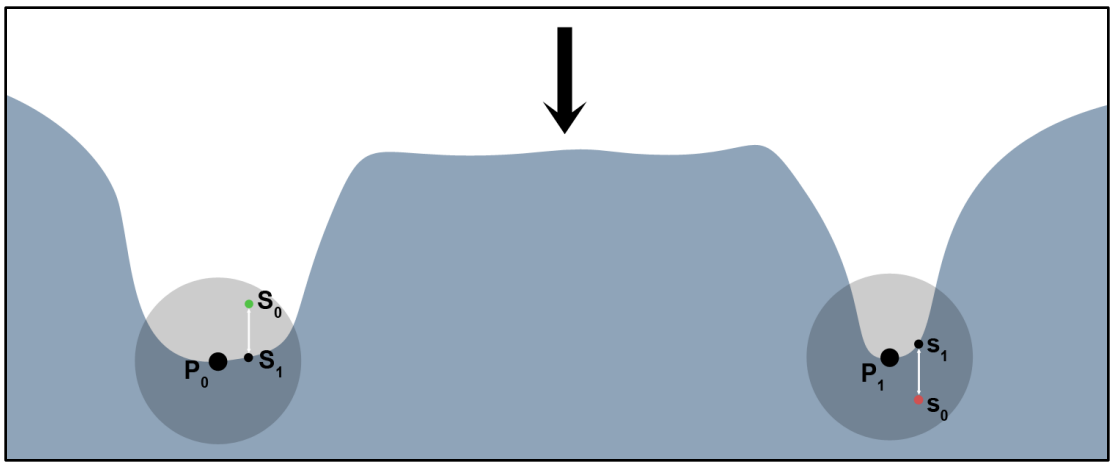

Figure 16: Illustrates the sampling and depth comparison process used in the ambient occlusion pass. The process is shown in 2D for clarity and the black arrow represents the camera viewing direction. The point P is the current pixel being processed. The sample point S_0 is the current sample point and the point S_1 is the surface position found in the depth buffer at the position of S_0. The white arrow illustrates the depth difference between the two samples. Point P_0 illustrates a scenario where the sample is found in front of the point. Point P_1 illustrates a scenario where the sample is found behind.

The text presented in the following three sections covering the three different ambient occlusion techniques share a common factor; they all describe the operation that takes place on a *single* pixel of the depth buffer (not counting the samples around the pixel for calculating the ambient occlusion). So the contents of each section describe a single iteration of the large loop mentioned in the previous paragraph, and for all techniques the process is then repeated for the total amount of pixels in the image.

4.3.1 Crytek Technique

The approach presented in this section is an adaption of the technique used in the computer game Crysis (Crytek 2007). More specifically, it is an adaption of the code presented in the book ShaderX7 (Kajalin 2009) by the original creator of the technique. By admission of the author himself, the code presented in the book is not the same as the production code used in the release version of Crysis, and some lines were changed or modified for the implementation here as well. As a consequence, the technique is not exactly the same as seen in Crysis; however, the end result is reasonably close and more importantly, it exhibits the same artefacts which makes it

less accurate than the Blizzard and Ray-Marching techniques. Figure 17 shows the three main artefacts that make the Crytek approach the least accurate technique. The function for computing ambient occlusion using this technique can be viewed in full in appendix A.

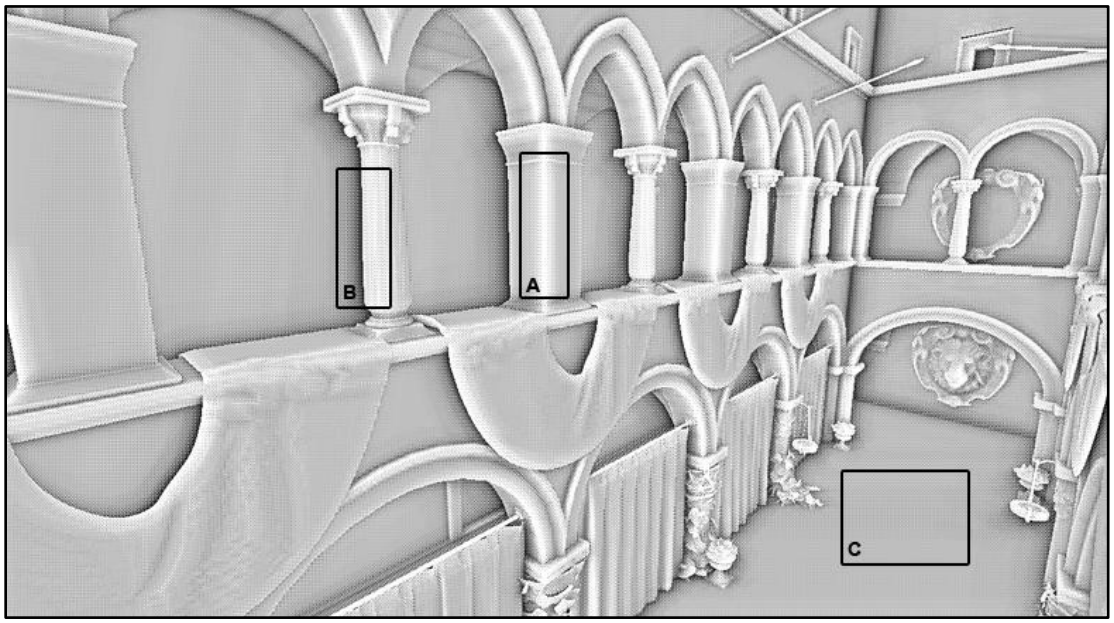

Figure 17: An example buffer of the Crytek ambient occlusion technique. Three major artefacts are present here; the edge highlighting (A); the pillars occluding (darkening) part of the wall behind which are too far away (B); and the occlusion of planar surfaces which should be unoccluded (C). The buffer shown here is not blurred.

4.3.1.1 Initialising Steps

The first step of the Crytek technique as well as the other two techniques surprisingly have nothing to do with ambient occlusion per se, but is a necessary step to circumvent certain limitations in the way the graphics card works. Essentially, all three ambient occlusion techniques presented need a random vector sampled from a texture; but using the unmodified texture coordinates of the pixel being processed to sample the random vector results in the distracting noise pattern on the left of figure 18. What is needed is a non-uniform sampling strategy for retrieving the vector, and this is handled by the following line of code:

```
float2 rotationTC = screenTC * screenSize / 4.0f;
```

The variable screenTC holds the texture coordinates of the current pixel while the screenSize variable holds the width and height of the current resolution. As is evident, the modified texture coordinates stored in rotationTC is scaled by one quarter of the screen resolution. The resulting modified (tiled) texture coordinates are used for retrieving the random vector from a pre-defined texture map handled by the following line of code:

```
float3 vRotation = 2 * tex2D(sRandVectSampler, rotationTC).rgb - 1;
```

The variable sRandVectSampler holds the texture map containing the random vectors (see figure 18 middle) from which a vector is retrieved and stored in vRotation. Since the vector is stored in the range of 0 to 1, the vector is transformed to the correct -1 to 1 range. Using the modified texture coordinates to non-uniformly sample the random vector is a very important step for all three techniques, and figure 18 on the right shows the result of using the modified coordinates.

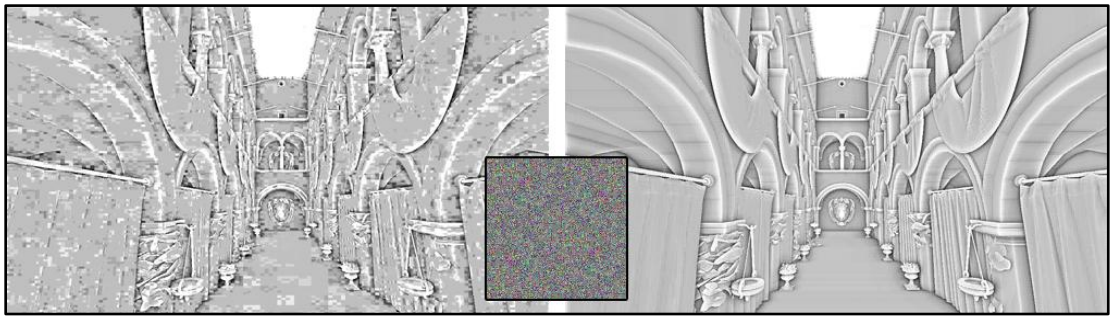

Figure 18: The result of tiling the texture coordinates used to sample the random vectors. On the left no tiling is used, while on the right tiling is used. The texture holding the random vectors is shown in the middle. The XYZ components of the vectors are stored in the RGB channels of the texture causing the coloured noise pattern.

The actual use of the random vector and the reason for this process will be explained shortly. Following the random vector sampling, the depth value at the current pixel is read from the depth buffer and stored in the variable fSceneDepthP and the occlusion factor is initialized to 0:

```
float fSceneDepthP = tex2D(sSceneDepthSampler, screenTC).r;
```

```
float fAccessibility = 0;
```

Note that in this technique the occlusion factor is actually called accessibility. Interestingly, this is more accurate terminology since the value being accumulated for each pixel is actually the accessibility and not the occlusion. One way to look at it is to consider that an accessibility value of 0 corresponds to a completely occluded point; while a value of 1 means that the point is completely unoccluded. In other words, accessibility is the inverse of occlusion.

4.3.1.2 Generating Samples

The next step is to sample a specified number of points around the current pixel position and accumulate the accessibility or occlusion factor, depending on how you look at it. For the Crytek technique this process is handled in a multi-nested loop shown in the following code sample:

```
for(int i = 0 ; i < (nSamplesNum/8) ; i++)
for(int x = -1 ; x <= 1 ; x += 2)
for(int y = -1 ; y <= 1 ; y += 2)
for(int z = -1 ; z <= 1 ; z += 2)
```

Until otherwise noted, the code samples in the following text are performed inside these loops. The variable nSamplesNum is set to the desired number of samples to generate around the current pixel position. The three inner loops go through the corners of the unit cube which is used in the following line of code to generate different offset vectors:

```
float3 vOffset = normalize(float3(x, y, z)) * offsetScale;
```

The variable offsetScale represents the variable d_{max} presented in section 3.3. This variable controls the radius of the sphere that samples are being generated in, and therefore the distance to which surfaces are taken into account for occlusion. As they

are, these vectors could be used to sample around the current pixel position, but this would result in the banding shown in figure 13 on page 28. To counteract this, the random vector sampled in the previously explained process is used to rotate the current offset vector:

```
float3 vRotatedOffset = mul(vOffset, matRotate);
```

The current offset vector is multiplied with a rotation matrix (matRotate) created from the randomly sampled vector, and since this vector is different for each pixel being processed; the end result is the jittering process described in section 2.1 and 3.5 giving the high frequency noise present on the right in figure 13. Each iteration of the loop structure generates a different offset vector, and during each iteration this vector is used to sample the depth at the position defined by this offset vector:

```
float3 vSamplePos = float3( screenTC, fSceneDepthP);

vSamplePos += float3( vRotatedOffset.xy, vRotatedOffset.z *
fSceneDepthP);

float fSceneDepthS = tex2D( sSceneDepthSampler, vSamplePos.xy);
```

First, the sample position is defined using the texture coordinates and the sampled pixel depth, which is just the position of the current pixel (P_0 and P_1 in figure 16). This position is then offset using the current offset vector and projected into the sphere using the pixel depth retrieved previously (S_0 in figure 16). This offset sample position is now located at a random point in the sphere around the position of the pixel currently being processed. Using the x and y coordinates of this position; the depth of the pixel that is stored in the depth buffer (S_1 in figure 16) can be retrieved and stored in the variable fSceneDepthS.

4.3.1.3 Calculating the Occlusion

At this point, all the values needed to compute the occlusion factor are ready, and the following conditional is evaluated:

```
if(fSceneDepthS >= 1.0f)
{
	fAccessibility += 1.0f;
}
else
{
	float fRangeIsInvalid = saturate(fSceneDepthP - fSceneDepthS);
	fAccessibility += lerp( fSceneDepthS > vSamplePos.z, 0.5f,
	fRangeIsInvalid );
}
```

If the depth of the sample point is equal to 1 (the furthest in the scene, since depth ranges from 0 to 1), the sample is discarded and contributes no occlusion. Otherwise, a value determining whether the sample is within range to act as an occluder is computed and stored in the fRangeIsInvalid variable. This variable is clamped between 0 and 1 using the saturate function, meaning that negative depth deltas are clamped to 0. Finally, the accessibility factor is accumulated in the fAccesibility variable using a linear interpolation between a default occlusion value of 0.5; and either 1 if the depth delta is positive or 0 if the depth delta is negative (sample is in front or behind respectively).

At this point, the loop is finished and the average accessibility factor is calculated in the following code sample:

```
fAccessibility = fAccessibility / nSamplesNum;
return saturate( fAccessibility * fAccessibility + fAccessibility);
```

The return statement includes an amplifying term to make the effect stronger; the saturate function is used to prevent values above 1.

4.3.2 Blizzard Technique

The Blizzard technique presented in this section was implemented based on the conceptual outline presented by (Filion and McNaughton 2008). The technique uses

the same tiling and sampling of a random vector as described in section 4.3.1, however, the whole process takes place in view-space instead of screen-space. The technique is still classified as a screen-space approach, but the sampling takes place in 3D, in view space. As with the Crytek technique, the source code for computing the ambient occlusion can be found in appendix B.

4.3.2.1 Initialising Steps

First, the depth of the current pixel is determined and then the view-space position of the pixel is determined:

```
float fPixelDepth = tex2D(sSceneDepthSampler, screenTC).r;

float3 vPixelPosViewSpace = fPixelDepth * frustumCorner;
```

The variable frustumCorner contains the view-space coordinates of the far corners of the camera frustum. When this variable is passed from the vertex shader to the pixel shader, the position gets interpolated which results in a ray pointing from the camera position to an interpolated position on the far clip plane. Because of the interpolation, this ray passes through the view-space position of the pixel, and multiplying with the pixel depth therefore gives the view-space position of the pixel.

Since this technique also uses the surface normal at the pixel position, the following code retrieves the normal and transforms it into view-space by multiplying with the inverse transpose of the camera view matrix. This matrix multiplication is important because all vectors used in the calculation must be in the same coordinate space for the technique to work correctly. The normals are stored in world-space and must therefore be transformed to view-space.

```
float3 vNormal = 2.0f * tex2D(sNormalSampler, screenTC) - 1.0f;

float3 vNormalView = mul(vNormal, InverseTransposeView);
```

4.3.2.2 Generating Samples

With the surface normal and pixel position determined, the technique enters a loop structure similar to the Crytek one, however; this time a sampling kernel containing vectors distributed in the unit sphere is used, instead of the corners of the unit cube. Consequently, no nested loop is required here, and a single loop is used to iterate through the number of specified samples:

```
for(int i = 0 ; i < NUM_SAMPLE_POINTS ; i++)
```

As in the Crytek technique a jittered offset vector is used for sampling. Instead of using a rotation matrix, the offset vector is generated by reflecting a vector from the previously mentioned unit sphere kernel, through the randomly sampled vector:

```
float3 vSampleOffset = reflect(pSphere[i], normalize(vRandomVector));
```

The vectors from the unit sphere kernel are of random length and so should not be normalized in this step. With the offset vector generated, a dot product is performed to check if the vector is inside the hemisphere oriented around the surface normal:

```
float RayDot = dot(normalize(vSampleOffset), vNormalView);
if (RayDot < 0)
      vSampleOffset = -vSampleOffset;
```

If the result of the dot product is negative, it means that the vector resides in the negative half-space of the unit sphere with regards to the surface normal. In other words, it is lying in the opposite hemisphere. In that case, the vector is flipped, effectively resulting in a doubling of the amount of sample points; the process is illustrated on the left in figure 19. In the Crytek technique, these samples found lying below the surface are considered occluders, which is obviously wrong, since the object is then occluding itself at all times.

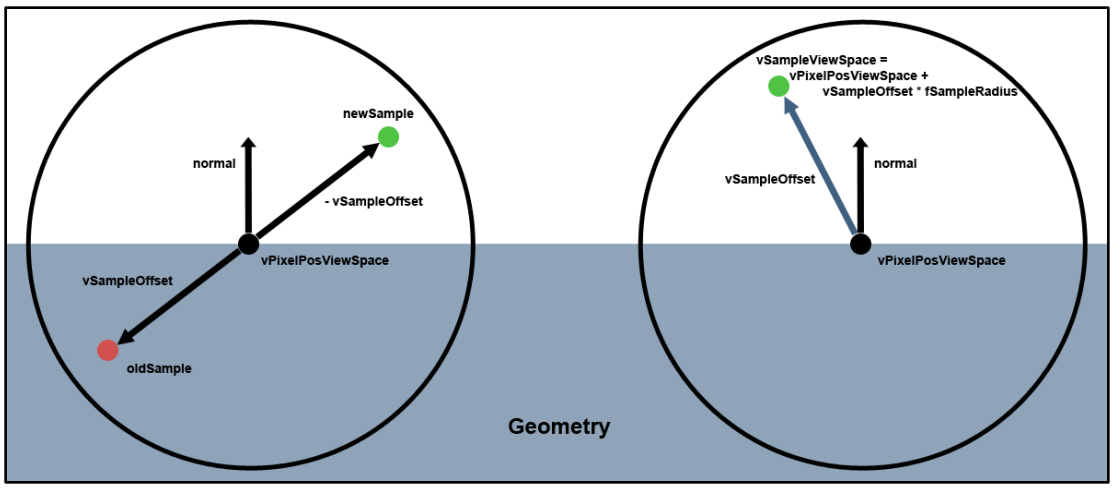

Figure 19: The sample process in view space. Shown on the left; the process of inverting the offset vector if it is found lying in the opposite hemisphere. Shown on the right; the process of generating the sample point using the offset vector.

With a proper offset vector, a sampling point is generated in view-space with the following code sample:

```
float4 vSampleViewSpace = float4(vPixelPosViewSpace + vSampleOffset
* fSampleRadius, 1.0f);
```

The offset vector is added to the original position and multiplied with the fSampleRadius variable corresponding to the d_{max} parameter. The process is illustrated on the right in figure 19. At this point the algorithm needs to sample the depth from the depth buffer at the position of the sample point (see figure 16 on page 36). However, because the sampling process is carried out in view-space, this step is not as straightforward as in the Crytek technique. To sample the depth buffer at the correct position, the current sample point must first be transformed into screen-space. This transformation is handled by the following lines of code:

```
float4 vSampleClipSpace = mul(vSampleViewSpace, Projection);

float2 fSampleTexCoord = 0.5f * vSampleClipSpace.xy /
vSampleClipSpace.w + float2(0.5f, 0.5f);

fSampleTexCoord.y = 1.0f - fSampleTexCoord.y;

fSampleTexCoord -= fHalfPixel;
```

First, the sample is transformed to clip space using the perspective projection matrix. Then the sample texture coordinates are calculated by doing a homogenous divide and transforming into the 0 to 1 range. Finally, the coordinates are flipped around the y-axis and the texture coordinates are aligned with the pixel coordinates. This process results in texture coordinates that can be used to sample the depth from the depth buffer:

```
float fSampleDepth = tex2D(sSceneDepthSampler, fSampleTexCoord).r;
```

4.3.2.3 Calculating the Occlusion

At this point, the occlusion factor can be calculated and stored in the fResult variable. Note that fResult is initialised to 0 which indicates full occlusion. In this technique, the occlusion is accumulated using a variable called fOcclusionFactor, however; like in the Crytek technique, what is actually being accumulated is the accessibility factor. The difference is only semantic, but it is mentioned to prevent confusion of the terms. To compute the occlusion factor, the depth delta between the pixel and sample depth is calculated:

```
float fDepthDelta = max(fSampleDepth - fPixelDepth , 0);
```

The max function returns the largest value of the two parameters, so if the depth delta is negative a value of 0 is returned. This depth delta is then used to calculate the occlusion factor using the following two lines of code:

```
float fOcclusionFactor = fDistanceScale * fDepthDelta;

fOcclusionFactor = 1.0f / (1.0f + fOcclusionFactor *
fOcclusionFactor);
```

The fDistanceScale holds the full depth of the scene (the distance from the near clip plane to the far clip plane). Because the technique uses linear depth stored in the 0 to 1 range, the depth delta is converted to scene unit scale by multiplying with the distance scale. This is a necessary step because the occlusion function in this

technique includes a quadratic attenuation of the distance to control the amount of occlusion. Without the distance scale, the attenuation is much too strong, resulting in no occlusion being calculated anywhere in the scene, i.e. a completely white occlusion buffer. Following the distance scale, the occlusion is calculated using the quadratic attenuation and the following conditional is evaluated to accumulate the occlusion factor:

```
if(fDepthDelta < fFullOccThreshold || fDepthDelta > fNoOccThreshold)
{
	fResult += 1.0f;
}
else
{
	fOcclusionFactor = pow(fOcclusionFactor, fOcclusionPow);
	fResult += fOcclusionFactor;
}
```

Two artistic variables (fFullOccThreshold and fNoOccThreshold) are used to limit the occlusion within a certain threshold. Since screen-space ambient occlusion is empirical and not physical, such artistic variables are commonly used to adjust the effect for a desired look. If the depth delta falls outside the range between these two variables, the point is considered completely unoccluded, i.e. it has an accessibility of 1. An exponential variable fOcclusionPow is used to further control the strength of the occlusion. As with the Crytek technique, the return value of the occlusion function is the mean of the accumulated occlusion across all samples:

```
return fResult / NUM_SAMPLE_POINTS;
```

For an example of the ambient occlusion buffer generated using this technique, see section 4.3.4.

4.3.3 Ray-Marching Technique

This section is a great deal shorter than the previous two. The reason is that the technique presented here is very similar to the Blizzard technique, using the same process of generating offset vectors and samples, using the same occlusion function, etc. To avoid redundancy, only the changes made to the Blizzard technique are outlined here. The ray-marching technique is based on an idea mentioned in an article by (Bavoil and Sainz 2009). The authors implement a brute force "ray-tracing" technique in image space (equivalent to screen-space), where the algorithm steps (marches) along the offset vector in image-space, sampling and comparing depths at each step. The ray-marching technique presented here does the same, only in view-space instead of screen-space. Figure 20 illustrates the ray-marching technique visually.

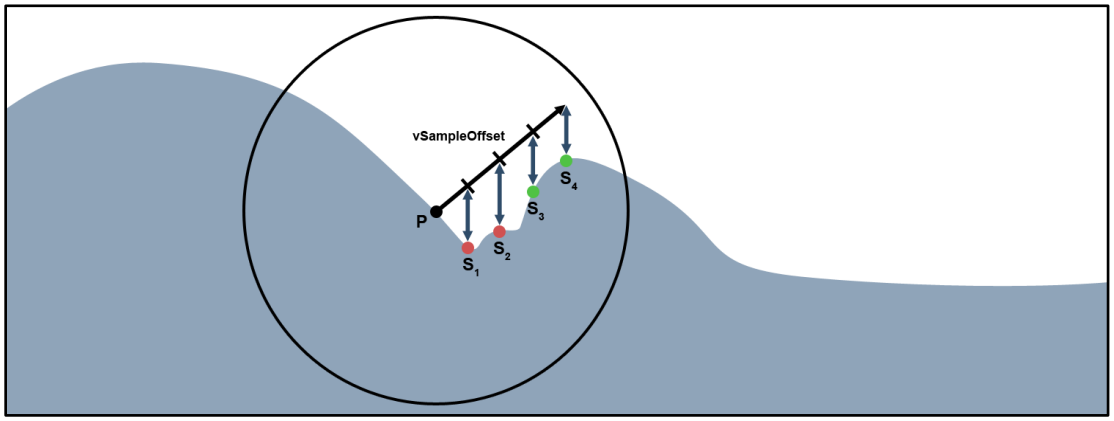

Figure 20: Illustrates the ray marching process. In the blizzard technique, the sample point is generated at the end of the offset vector, resulting in an occluder being found at sample S_4. Using ray-marching, the algorithm steps along the vector, sampling depths at each step. In this case, two non-occluding samples S_1 and S_2 are found, and then an occluding sample is found at S_3, closer than the occluder found by the Blizzard technique.

The benefit of using the ray-marching technique is that it is better at picking up detail than the Blizzard approach. The drawback is that it needs more samples in general to create good results. The need for more samples and the process of projecting and reading depth from a texture at each step means that this technique is slower than the Blizzard technique by a large margin. The following code is used to generate the offset vectors in the ray-marching technique:

```
float3 vStep = (1.0f / NUM_STEPS) * vSampleOffset * fSampleRadius;
```

Assuming that NUM_STEPS is set to 4, this generates an offset vector that is one quarter length of the original offset vector. The same transformation to screen-space and sampling of the depth buffer as in section 4.3.2 is performed and the depth delta is computed. If the following conditional evaluates to true, it means that no occluder was found at this step and the algorithm continues to the next step along the offset vector:

```
if(fDepthDelta < fFullOccThreshold)
```

The rest of the process is identical to the Blizzard technique, using the same function to accumulate the occlusion factor. The code for this technique can be found in appendix C. For an example of the occlusion buffer generated by this technique, see the following section.

4.3.4 Techniques Comparison and Discussion

This section reviews the three different techniques presented in the previous three sections, and discuss the differences between them. To begin with, figure 21 shows three ambient occlusion buffers generated using the three different techniques. The buffers are also included on the CD in full size for closer examination. As is evident from comparing the images in figure 21, the blizzard technique exhibits less problems with self-occlusion compared to the Crytek technique, particularly noticeable on the floor and the walls. The Blizzard technique also exhibits better detail than the Crytek one, most noticeable in the form of more intense occlusion in heavily occluded areas such as between the lower curtains and the arches. This is largely due to the better distribution of sample points in the Blizzard technique. While the Blizzard technique still exhibits edge highlighting to some degree, it is much more noticeable in the Crytek technique because of the relative brightness difference caused by the self-occlusion. When applied to a textured and lit scene, the edge highlighting is generally

not noticeable using the Blizzard technique, while it is noticeable using the Crytek one.

As mentioned in the previous section, the Ray-marching technique is better at picking up details than the Blizzard one (figure 20 illustrates why), and also exhibits less self-occlusion artefacts.

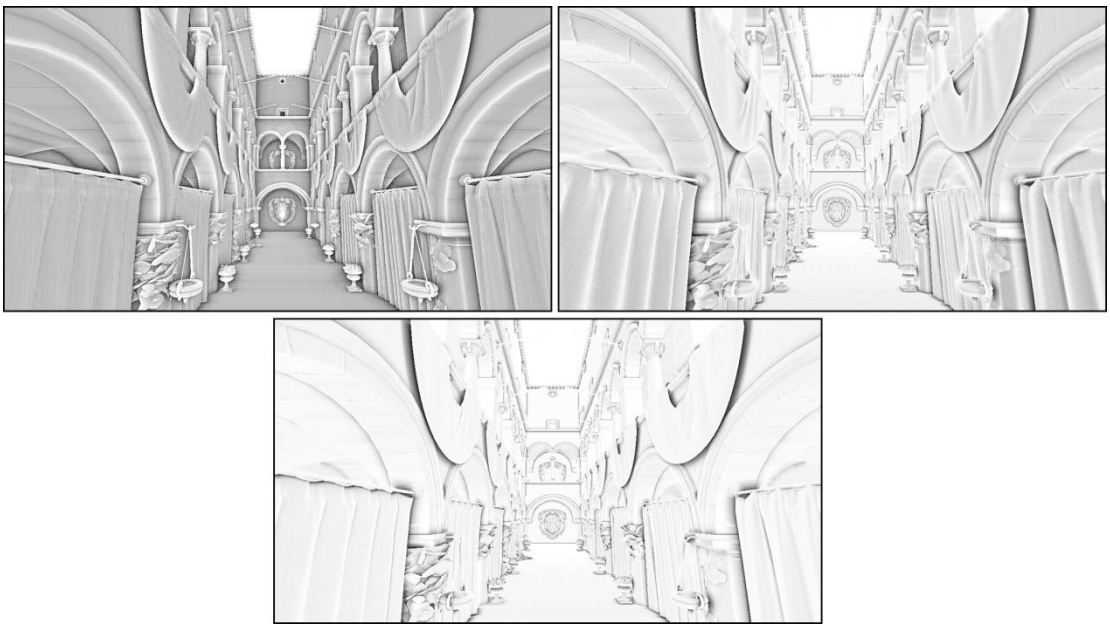

Figure 21: A comparison between the three different screen-space ambient occlusion techniques presented in this chapter. The upper left image shows the Crytek technique; the upper right shows the Blizzard technique; and the lower image shows the Ray-Marching technique.

4.4 Additional Implementation Considerations

This section outlines some additional details about the implementation that are relevant to the experimental study discussed in the next chapter. It was established in the introduction that one of the goals of the study is to investigate the perceptual effect of ambient occlusion in an ecologically valid scenario. In the context of this study, ecological validity implies that the techniques should be investigated in the context that they are most likely meant for; namely computer games. Consequently, ecological validity calls for experiment scenarios that visually mimic that of a

computer game in visual complexity. This not only impacts the design of the stimuli discussed in section 5.3, but also adds additional requirements to the rendering framework. To increase the ecological validity of the experiment stimuli, several additional features were added to the rendering framework including normal mapping, irradiance environment mapping, as well as support for rendering skyboxes. The high dynamic range lighting was implemented using a third party tone mapping class while the bi-lateral blurring of the occlusion buffers were handled using code adapted from (Bavoil and Sainz 2009).

These additional features combined with directional lighting and standard texture mapping allows for the creation of complex visual stimuli, mimicking the visual complexity of modern computer games. It is important to note that the goal of ecological validity in this study pertains primarily to the visual complexity of the *still* images presented. Obviously, the most ecologically valid scenario for performing a perceptual study examining these occlusion techniques would be an interactive setting such as a computer game, but the experimental approach in this study uses still images. The reasons for why are outlined in section 5.2.

All stimuli sets used in the experiment can be viewed in section 5.3 in the following chapter, in the appendix, as well as on the CD in full resolution.

Chapter 5: Experiment Procedure and Results

This chapter details the process of determining an experimental procedure that will assess the questions posed in section 1.2. The process of creating the stimuli for the experiment is also covered here, as well as details about the execution of the experiment. In the last two sections the results of the experiment are outlined and analysed.

The introduction outlined the research goal of this thesis in general terms, forming a motivational basis for the study. In the following section, the research goal is formulated in a more concise and structured manner, in the form of three experimental hypotheses.

5.1 Experimental Hypotheses

In general terms, the goal of this study is to investigate the perceptual influence of ambient occlusion on the perceived realism of synthetic images. Underlying this general inquiry, there are three distinct research questions that are addressed in the study. These questions are formally stated in three experimental hypotheses, outlined in table 3 in logical progression:

Table 3: The three experimental hypotheses investigated in the experiment.

Hypothesis 1: (H1)	The addition of ambient occlusion to a synthetic image will result in an increase in perceived realism by human observers
Hypothesis 2: (H2)	Increasing the physical accuracy of the ambient occlusion will result in a corresponding increase in perceived realism by human observers
Hypothesis 3: (H3)	The effect of ambient occlusion on perceived realism differs according to the complexity of the visual stimuli in which it is presented

All three hypotheses of course pertain to real-time rendering scenarios using screen-space ambient occlusion; although all three would be equally valid inquiries in an

offline rendering scenario using e.g. ray-traced ambient occlusion. The null hypothesis for H1 is that the addition of ambient occlusion will *not* increase the perceived realism; for H2, the null hypothesis is that increasing accuracy will *not* increase perceived realism; finally, for H3 the null hypothesis is that ecological validity has no bearing on ambient occlusion's effect on perceived realism.

5.2 Experiment Procedure

This section outlines the considerations behind the design of the experimental procedure used to investigate the experimental hypotheses outlined in the previous section. Several existing approaches to measuring visual realism in synthetic images were discussed in section 2.2 and this section builds on the observations made there.

A determining factor in this study is that it should possess a high level of ecological validity. Arguably, the most ecologically valid scenario would be to have experiment participants navigate a virtual environment freely, allowing them to experience the environment with and without ambient occlusion, as well as with occlusion techniques of different physical accuracy; all without allowing for any direct comparison. Participants would then perform a subjective evaluation of which scenario they found the most visually realistic. Unfortunately, this approach provides no guarantee that subjects perceive the same imagery, with the most extreme case being that their subjective evaluation are based on entirely different factors. Comparing results in such cases would be fruitless as they would possess no internal validity.

A compromise is needed between ecological and internal validity so that the results can be interpreted and generalised in a meaningful context. An acceptable compromise is to follow a no-reference approach using visually complex image pairs as stimuli. (Yu, et al. 2009) use five second videos as stimuli and using videos was initially considered for this experiment procedure as well. However, the cited experiment allows for direct and continuous comparison between the stimuli videos.

The no-reference approach adopted here does not allow for such direct comparison and as a consequence, the use of videos was ruled out. The reasoning behind this decision was that the temporal span of even very short videos would be too much for participants to retain and process without the possibility of direct comparison.

Using the approach of comparing image pairs, the stimuli can be presented in a more controlled albeit less ecologically valid manner, ensuring consistency between results. The choice of experimental approach in this study is thus very similar to the ones carried out by (Jimenez, Sundstedt and Gutierrez 2009) and (Sundstedt, et al. 2007). In more descriptive terms, experiment participants should be subjected to stimuli in the form of image pairs designed specifically for investigating the hypotheses outlined in the previous section; and then be tasked with performing a subjective evaluation following each image pair. By adopting this approach, stimuli that only change along one dimension can be designed providing a more controlled scenario with only one independent variable; either the presence or absence of ambient occlusion; or changing physical accuracy of the occlusion technique used. As a consequence, any patterns observed in the dependent variable (the perceived realism) should be due to these changing factors alone (Bartz, et al. 2008). This puts an emphasis on the importance of carefully designed stimuli pairs, which is the subject of the next section. One remaining crucially important part of the experiment procedure is the formulation of instructions for the experiment participants.

The approach outlined thus far requires participants to make a simple evaluation between two images, resulting in a binary choice. However, the manner in which participants are prompted to evaluate the images can exert great influence on participants' responses. The reason for this is that human perception is not driven by stimuli alone, but also by cognitive constraints such as goals and expectations (Palmer 1999, 13-14). Phrasing the instructions is thus a delicate balance; attempting to elicit the kind of responses from participants that will apply to the research in question, but without priming them and contaminating the results in the process.

To that end, a straightforward approach is to simply ask participants to choose the image they found the most realistic in visual appearance. This presents the problem of participants providing their own definition of visual realism. Defining realism for the participants in terms of lighting, shadows, etc., almost certainly constitutes a priming act which could influence the responses given. Simply asking about realism without an explicit definition does hold the risk of participants each having a different concept of realism (although unlikely) which could bias the results, but defining realism for the participants almost certainly will bias the results.

On the opposite end of the scale from defining realism for them, participants could be asked what image they found the most pleasing in visual quality, aesthetics, etc. However, this would likely introduce more bias to the results since the question is now entirely subjective, whereas visual realism tends to be defined on the basis of objective visual realism, e.g. how light behaves and interacts with surfaces in the real world. Following that logic, asking participants to evaluate images according to visual realism should impel them to examine the images in terms of what visual realism means in objective terms, without priming them by explicitly telling them what to look for. The written instructions can be viewed in appendix D or on the accompanying CD.

5.3 Creating the Experiment Stimuli

In order to investigate all three hypotheses listed in section 5.1, the stimuli have to be carefully designed. To enable testing of H3, three categories of scenarios were devised that differ in ecological validity:

- A contrived category with low ecological validity
- A category with moderate ecological validity
- A category with high ecological validity

Within each category, stimuli sets were created to enable investigation of H1 and H2. The following subsections detail the three categories and the stimuli sets that were created for them. To distinguish between the images of the stimuli sets, the technique names outlined in section 4.3 are used. In addition, the names are suffixed with a number representing the amount of samples used, e.g. Blizzard24 means that the Blizzard technique from section 4.3.2 was used with a sample frequency of 24. All the stimuli can and should be viewed on the CD in the original resolution; which is 1280x720. Enlarged (but not full sized) versions of the stimuli pairs can also be viewed in appendix E-K for convenience. Each figure in the following sections refers to the corresponding appendix section.

Because screen-space approaches to ambient occlusion are empirical and not physical, there is no right way to configure the techniques. As evident from the implementation details for each technique implemented, they all have different variables that can be adjusted and consequently change the appearance of the occlusion. Considerate effort was made to match the different techniques in appearance without compensating for any artefacts intrinsic to the technique. For example, no attempt was made to match the edge highlighting and self-occlusion of the Crytek technique when adjusting the Blizzard technique, but the sampling radius of both techniques were adjusted so that they would roughly affect the same area.

5.3.1 Low Ecological Validity

This category represents a contrived scenario that uses only a single object, with no illumination except for a constant ambient contribution of 1.

Figure 22: Low ecological validity. Crytek24 is shown on the left with Blizzard24 shown on the right. Larger versions can be found in appendix E.

The stimuli illustrated in figure 22 enables the investigation of H2 but not H1, however; rendering the dragon with constant ambient light and no ambient occlusion results in a completely flat render with the only shading coming from the texture map (see figure 9 on page 20). This scenario was deemed too trivial and so for this category only H2 is investigated.

5.3.2 Moderate Ecological Validity

To simulate a moderate level of ecological validity, stimuli sets were created using only indirect illumination. In contrast to the previous category, the indirect illumination is not constant but is instead sampled from an irradiance environment map. The environment maps were created so that they roughly correspond to the environment they are used in, with the end result being that the indirect light is a very coarse approximation of how light would be transported in a physical simulation. The stimuli sets also exhibit much greater visual complexity than the previous category.

Two different scenes were devised, one architectural and one involving virtual characters. The architectural scene uses a model of the Sponza Atrium courtesy of Crytek GmbH. The characters used are the main characters from the computer game "Resident Evil 5" courtesy of Capcom. The two scenes differ greatly in the visual

dominance of the ambient occlusion. For the architectural scene, the ambient occlusion is a moderately dominant feature as illustrated in figure 23.

Figure 23: Moderate ecological validity. No ambient occlusion is shown on the left with Blizzard24 shown on the right. Larger versions can be found in appendix F.

Figure 23 enables the investigation of H1. To investigate H2 in the context of moderate ecological validity, a second image pair was created shown in figure 24.

Figure 24: Moderate ecological validity. Crytek24 is shown on the left with Blizzard24 shown on the right. Larger versions can be found in appendix G.

For the characters, the ambient occlusion is much less dominant, primarily due to less spatial area showing the ambient occlusion, but also because the characters have a certain amount of occlusion pre-computed into their texture maps. Such pre-computation is a common approach in real-time rendering and is the primary reason for including these characters into the stimuli sets. Only one stimuli pair was created for the characters in this category and is shown in figure 25. This stimuli pair was included to investigate a large disparity in objective occlusion quality, evident by the techniques and sample quantities used.

Figure 25: Moderate ecological validity. Blizzard8 is shown on the left with RayMarching30 shown on the right. Note that much of the detail present in these renders come from the characters texture maps and not the ambient occlusion, e.g. the folds in the pants. Larger versions can be found in appendix H.

5.3.3 High Ecological Validity

To simulate a high level of ecological validity, the same two scenes from the previous section were used but with an added directional light. The addition of direct illumination makes the ambient occlusion less dominant visually and is closer to a real-world scenario than the previous category. Figure 26 shows the stimuli pair used to investigate H1.

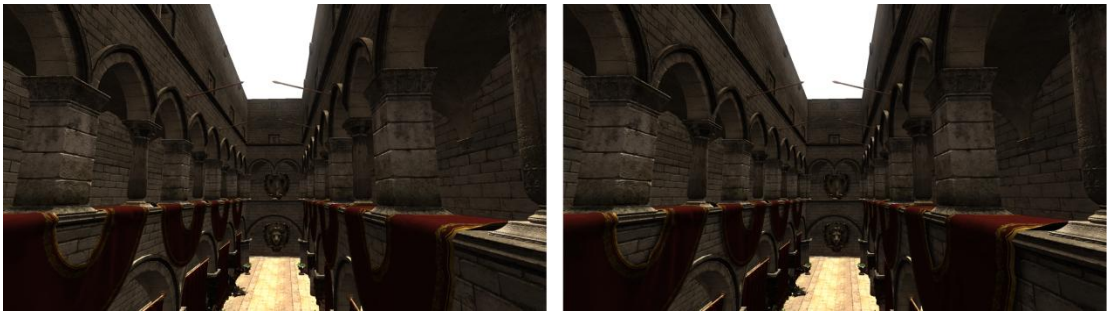

Figure 26: High ecological validity. No ambient occlusion is shown on the left with Blizzard24 shown on the right. Larger versions can be found in appendix I.

Like the moderate category a stimuli pair was also created to investigate H2, this pair is shown in figure 27.

Figure 27: High ecological validity. Crytek24 is shown on the left with Blizzard24 shown on the right. Larger versions can be found in appendix J.

One final stimuli pair was created for this category using the characters shown in the previous section. This stimuli pair was created for investigating H1 in a context of high ecological validity and is shown in figure 28.

Figure 28: High ecological validity. No ambient occlusion is shown on the left with Blizzard24 shown on the right. Again, much of the detail present in these renders come from the characters texture maps and not the ambient occlusion, e.g. the folds in the pants. Larger versions can be found in appendix K.

5.4 The Experiment

The experiment was carried out over the course of two days on the IHK campus in Ballerup, Copenhagen. A total of 36 participants were recruited (26 male and 10 female, age range: 18-56). The majority of experiment participants were Medialogy students ranging from the 2th to 10th semester, making the process of acquiring participants very much convenience sampling. The participants all reported having

normal or corrected-to-normal vision and were all naïve with respect to the experiment background and purpose.

The stimuli pairs were presented on a laptop with a 15.4" widescreen monitor and a resolution of 1280 x 800 pixels. Lighting was dimmed during the experiment so that participants could properly view the images without any distracting glare or contrast issues. In order to control the process of showing the stimuli and recording participant evaluations, a windows form application was created using the .NET framework. The application was created so that the whole experiment procedure was contained within the application, from displaying instructions and image pairs to participant evaluations and recording these evaluations. Figure 29 shows three screenshots from the application including the instructions and the recording of participant responses.

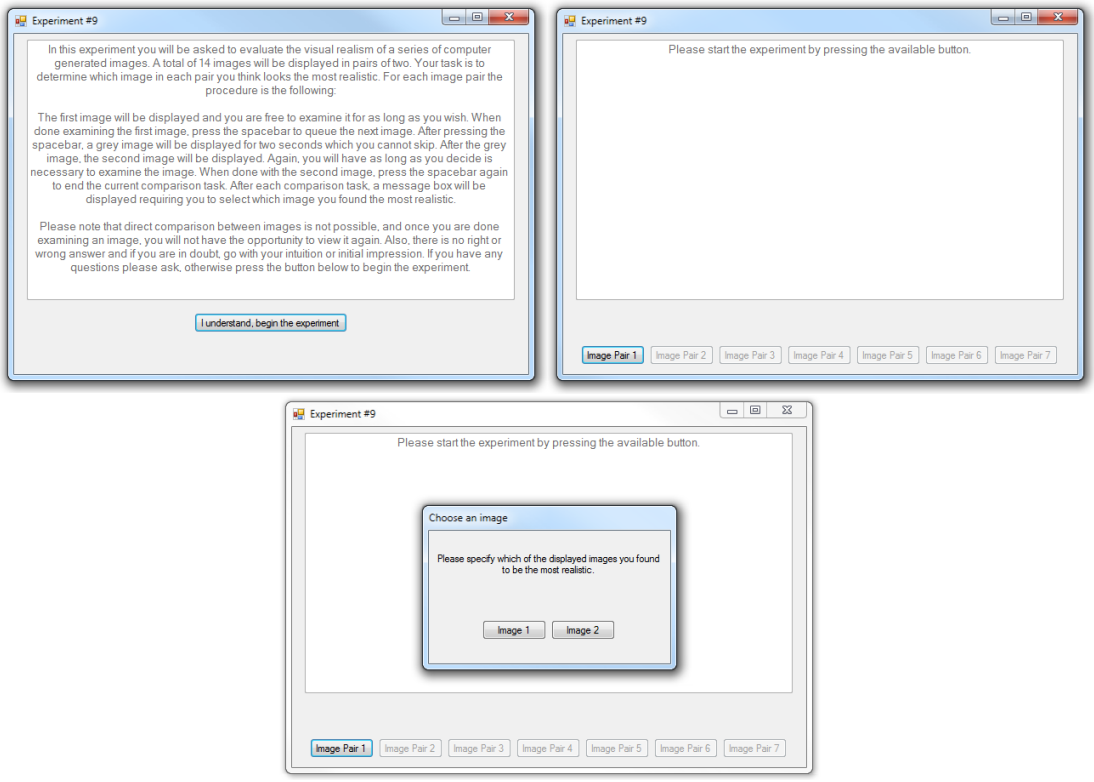

Figure 29: The experiment application used to display stimuli pairs and record participant responses. The application and source code is included on the accompanying CD.

The application was set up so that participants initiated each stimuli pair themselves by clicking the appropriate button in the interface (only one button is enabled at a

time), thus allowing participants to control the pace of the experiment themselves. By clicking the available image pair button, the first image of the current pair is shown and participants are given as much time as they deem necessary to examine the image. When done, participants were instructed to press the space bar to move on to the second image of the stimuli pair. In between the images, a mid-grey image was shown to prevent any direct comparison and to indicate the onset of the next image. Participants also controlled the time taken to examine the second image, and were then instructed to press the spacebar when done to initiate the evaluation step.

After each image pair, participants were asked to select which image looked the most realistic in a message box shown in the bottom of figure 29. Participants proceeded in this manner through all image pairs until done with the experiment.

Since the experiment procedure is a within-subject design, where each participant are subjected to all conditions (image pairs), the order of presentation is important. Simply presenting the same order to all participants could create order bias and randomising the order does not guarantee that the same condition will not appear e.g. first in several experiment runs. Instead, a Latin Square design was utilised to create different orders for each participant. Since there are a total of 7 conditions, a 7th order latin square was used to assign the conditions. However, since there are two images in each condition, the order within conditions should also be taken into account. To account for this, after 7 experiments have been run, the internal orders of the conditions are reversed and the latin square is run again. Once 14 experiments have been performed, a new latin square is generated for subsequent experiments. This process was handled internally and transparently in the experiment application.

Results were recorded automatically by the application and saved to a csv file for processing in Excel. The next section presents the results that were obtained from the experiment procedure.

5.5 The Results

In this section the results of the experiment are presented as is, with no analysis or discussion. The raw results of the csv file can be found on the CD. The results are presented here in order of the categories presented in section 5.3.

5.5.4 Low Ecological Validity Results

The only condition present in this category was the Stanford dragon (figure 22). In response to the stimuli, participants were evenly divided with 18 votes recorded in favour of the Crytek technique and 18 in favour of the Blizzard technique.

5.5.5 Moderate Ecological Validity Results

In the moderate category there were three conditions for evaluation. For the occlusion versus no-occlusion scenario (figure 23 page 57), 14 votes were recorded in favour of the no-occlusion scenario with 22 recorded in favour of the occlusion scenario. For the Crytek versus Blizzard scenario (figure 24 page 57), 11 votes were recorded in favour or the Crytek technique with 25 votes recorded in favour of the Blizzard one. For the characters (figure 25 page 58), the results were 16 votes for the Blizzard technique with 20 for the Ray-Marching technique.

5.5.6 High Ecological Validity Results

Three conditions were evaluated in the high category. For the no-occlusion versus occlusion scenario (figure 26 page 58), the results were 11 for no-occlusion and 25 for the Blizzard technique. For the Crytek versus Blizzard condition (figure 27 page 59), the results were evenly divided with 18 in favour of the Crytek technique, and 18 in favour of the Blizzard technique. For the last condition with the characters (figure

28 page 59), the results were 21 votes for the no-occlusion image, and 15 for the image with occlusion.

The results from the three previous sections are shown in chart form in the following figures. Figure 30 shows the results of the occlusion versus no-occlusion conditions investigating H1. Figure 31 shows the results of the Crytek versus Blizzard conditions investigating H2. Figure 32 shows the only condition involving the ray-marching technique also investigating H2.

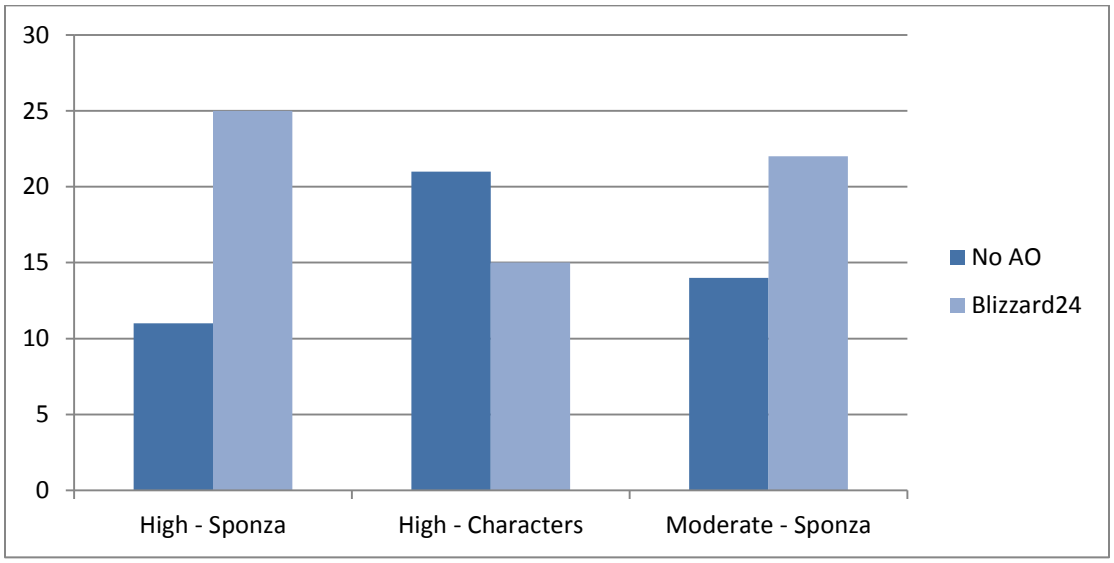

Figure 30: The results of the no-occlusion versus occlusion conditions. The Sponza label refers to the architectural scene with the high and moderate labels referring to the ecological validity.

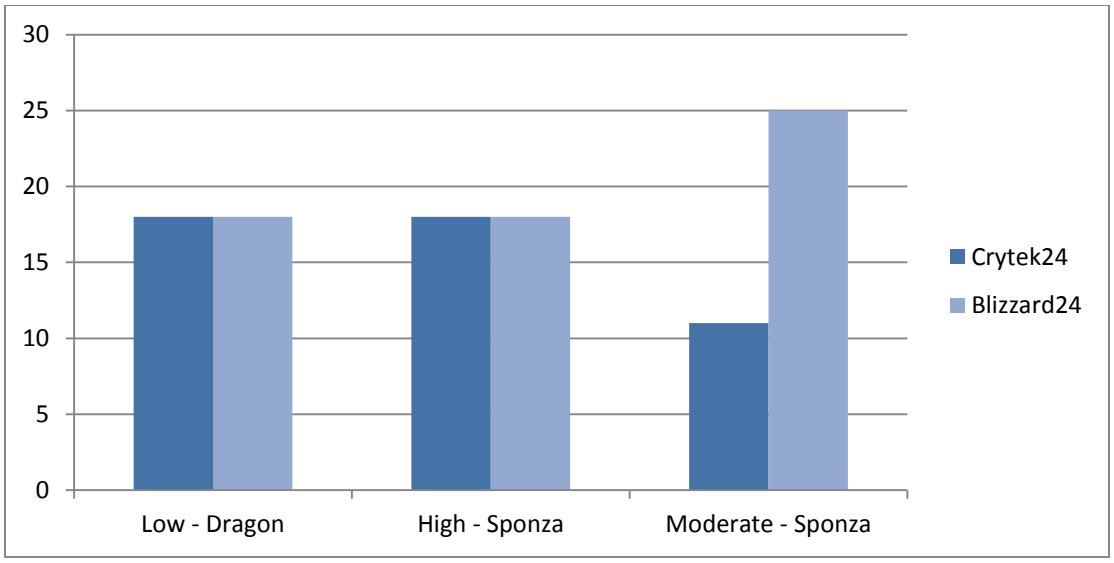

Figure 31: The results of the Crytek versus Blizzard conditions. The Sponza label refers to the architectural scene with the high and moderate labels referring to the ecological validity.

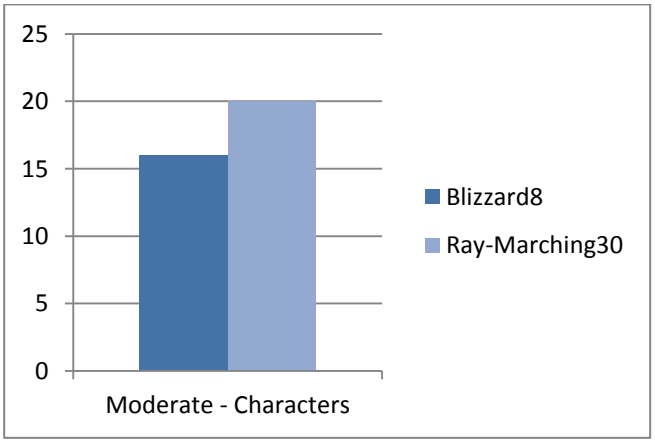

Figure 32: The results of the Blizzard versus Ray-Marching condition.

5.6 Statistical Analysis

A non-parametric technique called a Chi-Square was used to determine if there were any significance to the results, or if the distributions were what to expect by random chance (Jimenez, Sundstedt and Gutierrez 2009) (Sundstedt, et al. 2007). For each condition, the results were compared to an expected 18/18 distribution, indicating no

particular preference by experiment participants. The results of the Chi-Square test for all conditions are shown in table 4.

Table 4: The results of the Chi-Square test across all 7 conditions, bold numbers indicate a significant difference (p-value < 0.05).

Configuration	Chi-value (X^2)	p-value
Crytek24 / Blizzard24 (Low - Dragon)	0	1
No Occlusion / Blizzard24 (Moderate - Sponza)	1.778	0.182
Crytek24 / Blizzard24 (Moderate - Sponza)	**5.445**	**0.019**
Blizzard8 / Ray-Marching30 (Moderate - Characters)	0.445	0.505
No Occlusion / Blizzard24 (High - Sponza)	**5.445**	**0.019**
Crytek24 / Blizzard24 (High - Sponza)	0	1
No Occlusion / Blizzard24 (High - Characters)	1	0.317

The results from the dragon condition indicate either no preference or random guessing by participants. However, since the images are clearly perceptually different (see figure 22 page 56), it is more likely that participants had different preferences.

In the moderate validity condition (Sponza scene, figure 30 right), comparing no occlusion to the Blizzard technique, results indicate a small preference for the Blizzard technique although the results are not significant. This seem somewhat at odds with the results from the same comparison in the high validity category; which shows a significant preference for the Blizzard technique compared to the no occlusion image (figure 30 left). The comparison between the Crytek and Blizzard technique (Sponza scene, figure 31 right) in the moderate validity category shows a significant preference for the Blizzard technique while the results were evenly distributed in the high validity category (figure 31 middle).

In the moderate validity condition (characters, figure 32), comparing the ray-marching to the much lower quality Blizzard technique (sample frequency of 8), results show a slight preference for the ray-marching technique although the results from the Chi-square test indicate that this is due to random chance. Finally, for the high validity condition (characters, figure 30 middle), comparing no occlusion to the

Blizzard technique shows a small preference for the no occlusion image, but the result is not statistically significant. Of all the conditions included in the experiment, this is the only set of results that is completely inconsistent with the expected outcome. However, the images in this condition are perceptually very similar (see figure 28). Combining that observation with the statistical insignificance of the result makes the discrepancy likely to be random error.

Chapter 6: Discussion & Conclusion

This chapter contains the discussion and concluding remarks on the thesis as a whole. The discussion is written in a retrospective style, providing insights, comments, and critique on key elements of the thesis. The conclusion addresses the thesis goals and to what extent these goals were reached. Broader implications of the thesis findings are also treated in the conclusion. A brief section is included in the end with suggestions for future work.

6.1 Discussion

With the exception of the ray-marching versus Blizzard condition as well as the Stanford Dragon condition, the remainder of the results shows different levels of support for the hypotheses outlined in section 5.1. Comparisons between occlusion and no occlusion in the Sponza scene shows support for H1 in both the high and moderate validity category, although only the results from the high validity category are statistically significant. Comparisons between the Crytek and Blizzard techniques in the Sponza scene are a little more involved. Looking at the high validity category alone indicates that increasing physical accuracy does not increase perceived realism, however; the same comparison in the moderate category shows the opposite tendency. This outcome shows support for H3 and partial support for H2 in that the veracity of H2 appears to depend on the ecological validity of the scenario in which the comparison takes place. This particular observation also corresponds well with the findings by (Kozlowski and Kautz 2007); that approximations hold up better in more complex scenarios (see section 2.2).

6.1.1 Prominent Results

The most salient result of the experiment is the significant preference for ambient occlusion in the Sponza scene of the high validity category, and the complete lack of preference in the Crytek versus Blizzard condition also in the high validity category. The latter in particular is interesting, and stands in contradiction to the expectation formulated in H2. While the two techniques show strong objective differences in quality, and certainly also subjective when comparing the ambient occlusion buffers (see figure 21 on page 49), these differences are apparently not perceivable when integrated into a visually complex environment. Note that in this case, the images are perceptually similar and so I do believe that the even distribution is due to random chance, i.e. participants could not tell a difference. Considering that participants were not able to see a difference in the high validity category, it is perhaps tempting to disregard the importance of the fact that they were able to perceive a difference in the *moderate* category. However, the results from this condition still provide insight into what effect the accuracy of the ambient occlusion has in environments with little to no directional lighting. A scenario that comes to mind is an outdoor scene on an overcast day. In this scenario, the results intuitively point to higher quality ambient occlusion being an important factor on the perceived realism of the scene.

The patterns observed between the moderate and high validity categories in the Sponza scene shows a strong indication that ambient occlusion increases perceived realism in synthetic images in general. That might seem like a trivial observation, but ambient occlusion can vary greatly in the visual influence it has on an image. The high validity, no occlusion versus occlusion scenario using the characters (figure 30 middle, page 63) supports this observation. While the result of this condition shows a preference for no occlusion, I believe that this is due to random error and that a larger sample group would eventually converge towards an even distribution. Because of a limited spatial area for the ambient occlusion to operate on, coupled with the fact that the textures on the characters already exhibit a certain amount of occlusion, the effect of screen-space ambient occlusion in such a scenario are likely too subtle to notice in the absence of a reference image or prior knowledge of what to look for.

The results of the Stanford Dragon condition I believe to be due to poor stimuli design. I do not believe that the perfectly even distribution is because of participants guessing, but rather that participants had different preferences in this condition. Comments from a few participants' supports this observation, noting that they definitely could see a difference but were unsure which one was the 'right' one. This does highlight the inherent problem of asking people about perceived realism without providing an explicit definition for them. However, I do not believe this issue has contaminated all the results. Rather, the Dragon scenario does not provide a proper perceptual framework for evaluating it in terms of visual realism, due to missing lighting cues and the completely white background. In contrast, the Sponza scene while certainly not photorealistic does provide amble cues for participants to evaluate in terms of visual realism.

6.1.2 Stimuli Design

On the topic of the stimuli design, the scenario involving the characters were likely too subtle in their visual differences to be evaluated in the no-reference experiment design utilised in this study. Evaluating these image pairs in a direct comparison experiment could reveal different results than what was observed here. The question is what those kinds of results would actually show, other than human observers were able to tell the difference when given the opportunity to compare images directly. The choice of using a no-reference experiment design was a deliberate one because I do not believe allowing direct image comparison makes sense unless you are trying to match an approximating algorithm to a physical model.

One possible exception to this is the ordinal rank order experiment performed by (Yu, et al. 2009). Allowing participants to compare *all* images at the same time, from no occlusion to ray-marching, using different sampling frequencies, could provide some interesting results. Comparing two images when there is a clear perceptual difference

is a trivial exercise, but requesting participants to compare and rank a larger array of images could reveal some interesting patterns.

The adjustments made to the different occlusion techniques (mentioned in section 5.3) in creating the experiment stimuli means that the results observed from this experiment are not exhaustive. The experiment by (Yu, et al. 2009) shows that for ambient occlusion, the sampling radius can exert an effect on perceived realism. It is quite possible that increasing the occlusion radius and running the present experiment again using the altered stimuli would result in different observations. This highlights the importance of adjusting screen-space ambient occlusion appropriately to the given context, which is a common requirement for rendering techniques that are not physically based.

6.1.3 Experiment Procedure

As is often the case with studies of this type (Jimenez, Sundstedt and Gutierrez 2009) (Sundstedt, et al. 2007), the sample size is on the small side and the variety in experiment participants' background is limited. Perhaps the largest concern of utilising Medialogy students as the majority of test participants would be that they are in possession of certain knowledge giving them an advantage in comparing the image pairs. However, subjective responses from experiment participants indicated otherwise, as even participants with a background in some form of graphics, be it technical or design oriented, reported that many of the comparison tasks were quite difficult. On the topic of ecological validity, a more appropriate target group could be gamers, people with an interest in computer games. But a large part of the subjects that participated in this study already fits that description, if not in interest then at least in pertinent knowledge. In more precise words, I believe that a group of Medialogy students are more appropriate participants in this study than a completely arbitrary sample of individuals with a wide disparity in background knowledge and interests. With that said, an identical study on arbitrary individuals with no

proficiency or interest in computer games, computer graphics, or otherwise, could be interesting at the very least in an academic context. As always, for more accurate generalisation to a larger population, the sample size should preferably have been larger, but the experiment was able to generate a few significant results and provide interesting indications that should work well as motivators for a larger scale study.

The decision to use image pairs as the stimuli was done deliberately to enact a certain level of control over the experiment. While the results show interesting correlations between ambient occlusion and perceived realism, it is not known with any certainty if these observations generalise to a real-world scenario of e.g. a participant navigating a virtual environment. Unfortunately, performing such an experiment would mean that the experiment procedure would exact no control over what participants see, which would violate one of the most basic tenets of perception research (Bartz, et al. 2008). On their own, results from such a study would have little internal validity and any inferences from the results could depend on any number of factors. In conjunction with the study presented in this thesis however, correlation between results, if any, of the two studies could be investigated. While this approach would not provide a definitive answer, it could provide a strong indication for whether or not the results generalise to a real-world scenario.

6.1.4 Insights on Ambient Occlusion

I will make one last inference based on the results to conclude this discussion. The shift in importance of occlusion accuracy in going from moderate to high ecological validity highlights an important insight. The accuracy needed in ambient occlusion is directly related to the fidelity of all other aspects of the image such as lighting quality, texture resolution, surface detail, etc. The reason that the Crytek technique was sufficient in the high validity category is that it roughly matches the other elements of the scene in quality. The results of the study by (Yu, et al. 2009) are interesting in that in some cases, ambient occlusion ranked worse than no visibility for indirect

illumination at all. However in their context, visibility approximations were applied to physically accurate indirect illumination using four bounces. It makes intuitive sense to infer that in such a context, accuracy of the visibility approximations would matter more than in a real-time rendering scenario, using a coarse indirect light approximation in the form of an irradiance environment map. Put succinctly, more accurate indirect light simulations require more accurate visibility determination. And intuitively, higher graphics fidelity in other rendering aspects will likely lead to more strenuous accuracy requirements of the ambient occlusion technique used.

6.2 Conclusion

This thesis set out with the goal of investigating the perceptual influence of approximating ambient occlusion in real-time rendering scenarios. Three different screen-space ambient occlusion techniques of differing physical accuracy were implemented in an appropriate rendering framework with the purpose of investigating their effect on perceived realism of synthetic images. The ambient occlusion techniques together with a no occlusion scenario were investigated in a psychophysical study to ascertain whether the addition of ambient occlusion would increase perceived realism, and what effect the physical accuracy of ambient occlusion has on perceived realism.

The results show that, in visually complex stimuli rendered in a real-time context, ambient occlusion can have a significant effect on perceived realism. Furthermore, the results show that the complexity and nature of the image has an effect on the level of physical accuracy required of the ambient occlusion technique used. More specifically, observations from the results point to an inverse relationship between ambient occlusion accuracy and visual complexity; in that as visual complexity increases, the accuracy required of the ambient occlusion decreases. However, results also indicate that higher overall image fidelity in e.g. lighting would increase the required accuracy of ambient occlusion.

6.2.5 Broader Implications and Thesis Contribution

The broader implication and main contribution of the results is the suggestion of an upper threshold of required physical accuracy of ambient occlusion. This threshold is determined by the overall visual fidelity of the context in which the ambient occlusion is applied. Considering that screen-space ambient occlusion is an expensive computational process, even on current generation hardware, it would be prudent for computer game developers to run some rudimentary psychophysical experiments to determine where that threshold lies in the current rendering context. Findings of such experiments could highlight scenarios where the accuracy of the ambient occlusion could be toned down or even turned off completely, in order to dedicate computational resources to more perceptually important rendering tasks. The opposite could of course also be the case, and would then show a need for increasing the accuracy of the ambient occlusion to improve perceived realism.

In conclusion, screen-space ambient occlusion can have a significant effect on perceived realism of images rendered in real-time, but scenarios do exist where ambient occlusion can be very coarsely approximated or in some cases completely discarded. Performing a psychophysical study similar to the one presented in this thesis will allow developers to identify such scenarios and take action accordingly. Given that current generation graphics hardware, while very fast, still have limited computational resources; such a perceptually driven approach can assist in increasing perceived realism in real-time rendering.

6.3 Future Work

There are quite a few avenues of inquiry that could expand on the experimental approach and results presented in this thesis. Arguably the most pertinent avenue would be to transfer the experimental approach to an actual real-time environment. If the results of such a study correlate with the results presented here, a more definitive

answer could be provided on whether the findings of this thesis generalises to a real-time environment.

A large scale version of the experiment presented in this thesis could also be conducted to address the small sample size of the present study. The main purpose of this would be to investigate any changes in the results that were not found statistically significant, by using a larger population sample. The opportunity could also be leveraged to recruit a better defined target group of participants.

Finally, to further increase the ecological validity of the eventual results of the two cases mentioned here, different experimental stimuli could be utilised. An appropriate way to do this would be to find a current generation game engine that supports the writing of custom shaders, and then implement the different ambient occlusion techniques in that engine for generating the experiment stimuli. This approach would generate more ecologically valid stimuli that together with an increased sample size of a larger scale experiment could provide more accurate and statistically significant results.

Appendix A: Crytek Ambient Occlusion Code

```
float ComputeSSAO(float2 screenTC)
{
	//Tile the texture coordinates
	float2 rotationTC = screenTC * screenSize / 4.0f;

	//Sample a random vector and transform it into [-1, 1] range
	float3 vRotation = 2.0f * tex2D(sRandVectSampler,
	rotationTC).rgb - 1.0f;

	//Create rotation matrix
	float3x3 matRotate;
	float h = 1.0f / (1.0f + vRotation.z);
	matRotate._m00 = h * vRotation.y * vRotation.y + vRotation.z;
	matRotate._m01 = -h * vRotation.y * vRotation.x;
	matRotate._m02 = -vRotation.x;
	matRotate._m10 = -h * vRotation.y * vRotation.x;
	matRotate._m11 = h * vRotation.x * vRotation.x + vRotation.z;
	matRotate._m12 = -vRotation.y;
	matRotate._m20 = vRotation.x;
	matRotate._m21 = vRotation.y;
	matRotate._m22 = vRotation.z;

	//Specify number of samples
	const int nSamplesNum = 24;

	//Sample the depth at the current pixel
	float fSceneDepthP = tex2D(sSceneDepthSampler, screenTC).r;

	//Set the offset scale step
	float fOffsetScaleStep = 1.0f + 2.4f / nSamplesNum;

	//Initialize the accessibility factor to zero
	float fAccessibility = 0;

	//Sample area around current pixel and accumulate the
	accessibility factor
	for(int i = 0 ; i < (nSamplesNum/8) ; i++)
	for(int x = -1 ; x <= 1 ; x += 2)
	for(int y = -1 ; y <= 1 ; y += 2)
	for(int z = -1 ; z <= 1 ; z += 2)
	{
		//Create offset vector
		float3 vOffset = normalize(float3(x, y, z)) *
		(offsetScale *= fOffsetScaleStep);

		//Rotate the offset vector
		float3 vRotatedOffset = mul(vOffset, matRotate);

		//Center pixel's coordinates in screen space
		float3 vSamplePos = float3( screenTC, fSceneDepthP);


		//Offset sample point
```

```
            vSamplePos += float3( vRotatedOffset.xy, vRotatedOffset.z
            * fSceneDepthP);

            //Read sample point depth
            float fSceneDepthS = tex2D( sSceneDepthSampler,
            vSamplePos.xy);

            //Discard if depth equals max
            if(fSceneDepthS >= 1.0f)
            {
                  fAccessibility += 1.0f;
            }
            else
            {
                  //Compute accessibility factor
                  float fRangeIsInvalid = saturate(fSceneDepthP -
                  fSceneDepthS);

                  fAccessibility += lerp( fSceneDepthS >
                  vSamplePos.z, 0.5f, fRangeIsInvalid );
            }
      }

      //Compute average accessibility
      fAccessibility = fAccessibility / nSamplesNum;

      //Amplify and return the ambient occlusion coefficient
      return saturate( fAccessibility * fAccessibility +
      fAccessibility);
}
```

Appendix B: Blizzard Ambient Occlusion Code

```
float ComputeSSAO(float2 screenTC, float3 frustumCorner)
{

float fResult = 0;

//Offset the texture coordinates for sampling the random reflection
vector
float2 fOffsetTC = screenTC * fScreenSize / 4.0f;

//Sample the depth at the current pixel
float fPixelDepth = tex2D(sSceneDepthSampler, screenTC).r;

//Compute view (eye) space position of the pixel
float3 vPixelPosViewSpace = -fPixelDepth * frustumCorner;

//Sample a random vector to reflect offset vector
float3 vRandomVector = 2.0f * tex2D(sRandVectSampler, fOffsetTC) -
1.0f;

//Sample pixel normal and transform to view space
float3 vNormal = 2.0f * tex2D(sNormalSampler, screenTC) - 1.0f;

float3 vNormalView = mul(vNormal, InverseTransposeView);

//Sample area around current pixel and accumulate the occlusion
factor
for(int i = 0 ; i < NUM_SAMPLE_POINTS ; i++)
{
      //Reflect the sample offset vector through the random vector
      float3 vSampleOffset = reflect(pSphere[i],
      normalize(vRandomVector));

      //Flip if not inside the hemisphere (conditional is faster than
      using the intrinsic sign() function)
      float RayDot = dot(normalize(vSampleOffset), vNormalView);
      if (RayDot < 0)
            vSampleOffset = -vSampleOffset;

      //Compute the view space position of the sample point and
      transform to clip space
      float4 vSampleViewSpace = float4(vPixelPosViewSpace +
      vSampleOffset * fSampleRadius, 1.0f);

      float4 vSampleClipSpace = mul(vSampleViewSpace, Projection);

      //Calculate the texture coordinates of the sample in clip space
      (convert from [-1, 1] range to [0, 1])
      float2 fSampleTexCoord = 0.5f * vSampleClipSpace.xy /
      vSampleClipSpace.w + float2(0.5f, 0.5f);

      //Flip around the y-coordinate and align texels to pixels
      fSampleTexCoord.y = 1.0f - fSampleTexCoord.y;
      fSampleTexCoord -= fHalfPixel;
```

```
            //Read the depth of the current sample point from the
            depth buffer
            float fSampleDepth = tex2D(sSceneDepthSampler,
            fSampleTexCoord).r;

            //Calculate the occlusion factor of the current sample
            float fDepthDelta = max(fSampleDepth - fPixelDepth , 0);

            //Compute the occlusion factor. Scale to scene size so
            quadratic attenuation can be used
            float fOcclusionFactor = fDistanceScale * fDepthDelta;

            fOcclusionFactor = 1.0f / (1.0f + fOcclusionFactor *
            fOcclusionFactor);

            if(fDepthDelta < fFullOccThreshold || fDepthDelta >
            fNoOccThreshold)
            {
            fResult += 1.0f;
            }
            else
            {
                  fOcclusionFactor = pow(fOcclusionFactor,
                  fOcclusionPow);
                  fResult += fOcclusionFactor;
            }
      }
      return fResult / NUM_SAMPLE_POINTS;
}
```

Appendix C: Ray-Marching Ambient Occlusion Code

```
float ComputeSSAO(float2 screenTC, float3 frustumCorner)
{
float fResult = 0;

//Offset the texture coordinates for sampling the random reflection
vector
float2 fOffsetTC = screenTC * fScreenSize / 4.0f;

//Sample the depth at the current pixel
float fPixelDepth = tex2D(sSceneDepthSampler, screenTC).r;

//Compute view (eye) space position of the pixel
float3 vPixelPosViewSpace = -fPixelDepth * frustumCorner;

//Sample a random vector to reflect offset vector
float3 vRandomVector = 2.0f * tex2D(sRandVectSampler, fOffsetTC) -
1.0f;

//Sample pixel normal and transform to view space
float3 vNormal = 2.0f * tex2D(sNormalSampler, screenTC) - 1.0f;

float3 vNormalView = mul(vNormal, InverseTransposeView);

//Sample area around current pixel and accumulate the occlusion
factor
for(int i = 0 ; i < NUM_SAMPLE_DIRS ; i++)
{
float fDepthDelta = 0;

//Reflect the sample offset vector through the random vector
float3 vSampleOffset = reflect(pSphere[i], normalize(vRandomVector));

//Flip if not inside the hemisphere (conditional is faster than using
the intrinsic sign function)
float RayDot = dot(normalize(vSampleOffset), vNormalView);
      if (RayDot < 0)
            vSampleOffset = -vSampleOffset;

//Compute the step vector
float3 vStep = (1.0f / NUM_STEPS) * vSampleOffset * fSampleRadius;

//Step One of four
//Compute the view space position of the sample point and transform
to clip space
float4 vSampleViewSpace = float4(vPixelPosViewSpace + vStep, 1.0f);

float4 vSampleClipSpace = mul(vSampleViewSpace, Projection);

//Calculate the texture coordinates of the sample in clip space
(convert from [-1, 1] range to [0, 1])
float2 fSampleTexCoord = 0.5f * vSampleClipSpace.xy /
vSampleClipSpace.w + float2(0.5f, 0.5f);
```

```
//Flip around the y-coordinate and align texels to pixels
fSampleTexCoord.y = 1.0f - fSampleTexCoord.y;
fSampleTexCoord -= fHalfPixel;

//Read the depth of the current sample point from the depth buffer
float fSampleDepth = tex2D(sSceneDepthSampler, fSampleTexCoord).r;

fDepthDelta = max(fSampleDepth - fPixelDepth , 0);

//Step Two of four
if(fDepthDelta < fFullOccThreshold)
{
//Compute the view space position of the sample point and transform
to clip space
vSampleViewSpace = float4(vSampleViewSpace + vStep, 1.0f);
vSampleClipSpace = mul(vSampleViewSpace, Projection);

//Calculate the texture coordinates of the sample in clip space
(convert from [-1, 1] range to [0, 1])
fSampleTexCoord = 0.5f * vSampleClipSpace.xy / vSampleClipSpace.w +
float2(0.5f, 0.5f);

//Flip around the y-coordinate and align texels to pixels
fSampleTexCoord.y = 1.0f - fSampleTexCoord.y;
fSampleTexCoord -= fHalfPixel;

//Read the depth of the current sample point from the depth buffer
fSampleDepth = tex2D(sSceneDepthSampler, fSampleTexCoord).r;

fDepthDelta = max(fSampleDepth - fPixelDepth , 0);
}

//Step Three of four
if(fDepthDelta < fFullOccThreshold)
{
//Compute the view space position of the sample point and transform
to clip space
vSampleViewSpace = float4(vSampleViewSpace + vStep, 1.0f);
vSampleClipSpace = mul(vSampleViewSpace, Projection);

//Calculate the texture coordinates of the sample in clip space
(convert from [-1, 1] range to [0, 1])
fSampleTexCoord = 0.5f * vSampleClipSpace.xy / vSampleClipSpace.w +
float2(0.5f, 0.5f);

//Flip around the y-coordinate and align texels to pixels
fSampleTexCoord.y = 1.0f - fSampleTexCoord.y;
fSampleTexCoord -= fHalfPixel;

//Read the depth of the current sample point from the depth buffer
fSampleDepth = tex2D(sSceneDepthSampler, fSampleTexCoord).r;

fDepthDelta = max(fSampleDepth - fPixelDepth , 0);
}

//Step Four of four
```

```
if(fDepthDelta < fFullOccThreshold)
{
//Compute the view space position of the sample point and transform
to clip space
vSampleViewSpace = float4(vSampleViewSpace + vStep, 1.0f);
vSampleClipSpace = mul(vSampleViewSpace, Projection);

//Calculate the texture coordinates of the sample in clip space
(convert from [-1, 1] range to [0, 1])
fSampleTexCoord = 0.5f * vSampleClipSpace.xy / vSampleClipSpace.w +
float2(0.5f, 0.5f);

//Flip around the y-coordinate and align texels to pixels
fSampleTexCoord.y = 1.0f - fSampleTexCoord.y;
fSampleTexCoord -= fHalfPixel;

//Read the depth of the current sample point from the depth buffer
fSampleDepth = tex2D(sSceneDepthSampler, fSampleTexCoord).r;

fDepthDelta = max(fSampleDepth - fPixelDepth , 0);
}
//Calculate the occlusion factor of the current sample
float occlusionFactor = (fDistanceScale * fDepthDelta);
occlusionFactor = 1.0f / (1.0f + occlusionFactor * occlusionFactor);

if(fDepthDelta < fFullOccThreshold || fDepthDelta > fNoOccThreshold)
      fResult += 1.0f;
else
{
      occlusionFactor = pow(occlusionFactor, fOcclusionPow);
      fResult += occlusionFactor;
}
}
      return fResult / NUM_SAMPLE_DIRS;
}
```

Appendix D: Experiment Instructions

In this experiment you will be asked to evaluate the visual realism of a series of rendered images. A total of 14 images will be displayed in pairs of two. Your task is to determine which image in each pair you think looks the most realistic. For each image pair the procedure is the following:

The first image will be displayed and you are free to examine it for as long as you wish. When done examining the first image, press the spacebar to queue the next image. After pressing the spacebar, a grey image will be displayed for two seconds which you cannot skip. After the grey image, the second image will be displayed. Again, you will have as long as you decide is necessary to examine the image. When done with the second image, press the spacebar again to end the current comparison task. After each comparison task, a message box will be displayed requiring you to select which image you found the most realistic.

Please note that direct comparison between images is not possible, and once you are done examining an image, you will not have the opportunity to view it again. Also, there is no right or wrong answer and if you are in doubt, go with your intuition or initial impression. If you have any questions please ask, otherwise press the button below to begin the experiment.

Appendix E: Stimuli Pair I – Dragon Low

Crytek24

Blizzard24

Appendix F: Stimuli Pair II – Sponza Moderate

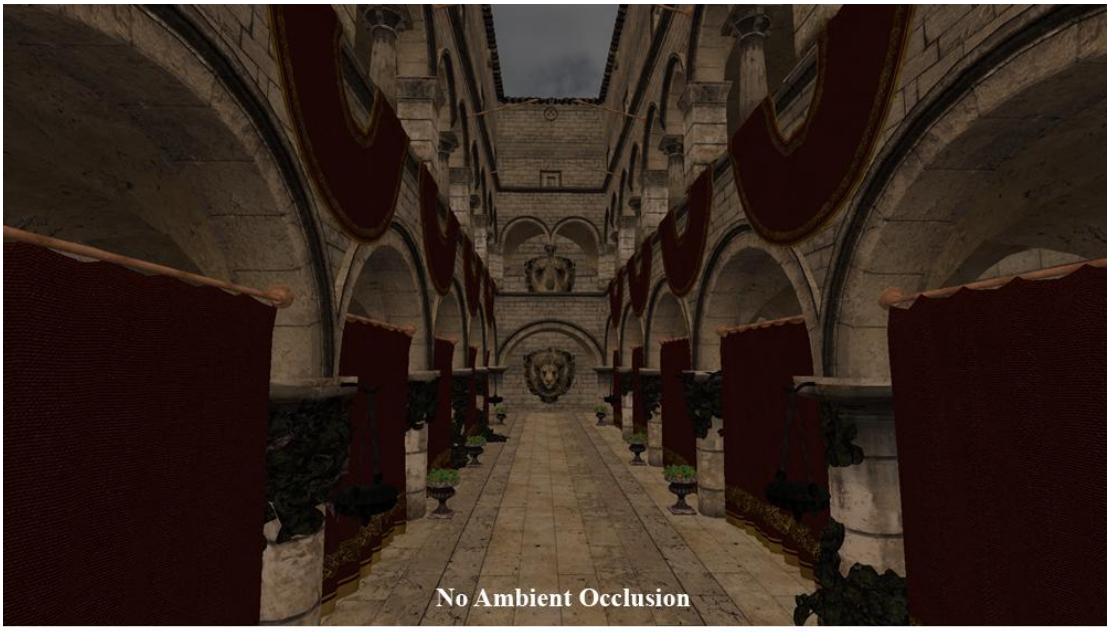

Appendix G: Stimuli Pair III – Sponza Moderate

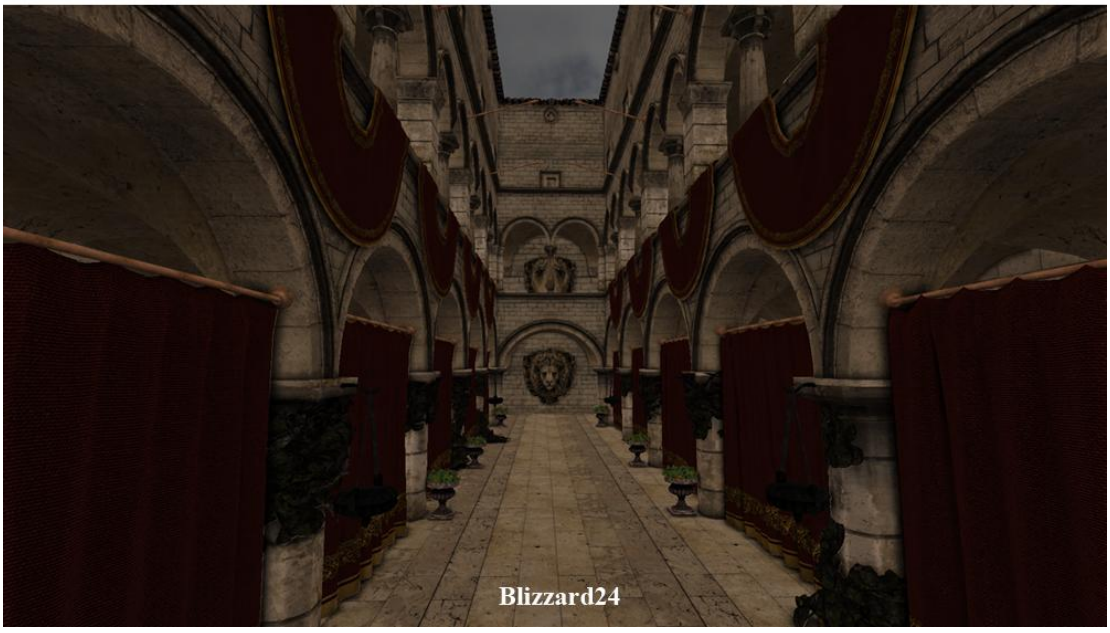

Appendix H: Stimuli Pair IV – Characters Moderate

Appendix I: Stimuli Pair V – Sponza High

Appendix J: Stimuli Pair VI – Sponza High

Appendix K: Stimuli Pair VII – Characters High

Glossary

Acceleration Structure: A programmatic construct used to partition the geometry of a scene into sections. Intersection tests with rays can then be performed on these top-level sections to determine if the ray intersects geometry contained within the section. If no intersection is found, all the geometry inside the section is skipped, speeding up intersection testing greatly.

Bidirectional reflectance distribution function: A function describing how light is reflected from a surface. Two directions are used in the function, the incoming light direction and the outgoing view direction.

Depth Buffer: A buffer holding the depth of all visible pixels.

Gold Standard: A reference image used to compare approximations with in psychophysical experiments. It is usually a real-world image or a physically accurate synthetic rendering.

Ground Truth: See Gold standard.

Irradiance: A measure of light incoming to a point from all directions in the hemisphere

Irradiance Environment Mapping: The process of using a heavily blurred environment map representing the scene to calculate irradiance. The process results in more shading variation in the indirect lighting than using a constant ambient light.

Jittering: Commonly defined as small rapid variations in a waveform. In the context of graphics programming, it is often used to indicate the process of creating a high-frequency random distribution of samples.

Lambertian Diffuse: A perfectly diffuse surface where light is scattered evenly in all directions.

Normal Mapping: A subset of bump mapping where modified normals are stored in a texture map which are then used in lighting calculations instead of the actual surface normals. This process results in shading that mimics geometry which is not actually there, creating additional surface detail.

Object-Space: 3D coordinate space. Object-space is defined locally for each object meaning that the origin is defined in some relation to a point on the object, e.g. the pelvis of a character model.

Radiance: A measure of light in a single ray

Screen-Space: The coordinate space after the 3D scene has been projected to 2D. The X and Y coordinates can be used with the Z-value from the depth buffer to reconstruct world- or view-space 3D positions.

Spherical Proxy: An approximate reconstruction of the surface underlying the sample pixel using a sphere. Can either be actual geometry or a mathematical construct used in an equation.

Surface Normal: A vector standing perpendicular to a surface, usually just referred to as the normal.

View-Space: Coordinate space relative to the virtual camera. The world-space coordinates are transformed so that the camera is placed at the origin and is looking down the z-axis into the scene.

World-Space: 3D coordinate space that defines where objects are placed and oriented in relation to each other.

This page is intentionally left blank.

Bibliography

Bartz, Dirk, Douglas Cunningham, Jan Fischer, and Christian Wallraven. “The Role of Perception for Computer Graphics.” *Proceedings of the 29th Annual Conference Eurographics.* Oxford, United Kingdom: The Eurographics Association, 2008. 65-86.

Bavoil, Louis, and Miguel Sainz. “Image-Space Horizon-Based Ambient Occlusion.” In *ShaderX7*, by Wolfgang Engel, 425-444. Boston, MA: Course Technology, 2009.

Cook, Robert L., and Kenneth E. Torrance. “A Reflectance Model for Computer Graphics.” *International Conference on Computer Graphics and Interactive Techniques.* Dallas, Texas: ACM, 1981. 307-316.

Crytek. *Crysis.* Frankfurt, November 2007.

Daly, Scott. “The Visible Differences Predictor: An Algorithm for the Assessment of Image Fidelity.” In *Digital Images and Human Vision*, by Andrew B. Watson, 179-206. Cambridge, Massachusets: MIT Press, 1993.

Filion, Dominic, and Rob McNaughton. "StarCraft II - Effects & techniques." *International Conference on Computer Graphics and Interactive Techniques.* Los Angeles: ACM, 2008. 133-164.

Goral, Cindy M, Kenneth E Torrance, Donald P Greenberg, and Bennet Battaile. “Modeling the Interaction of Light Between Diffuse Surfaces.” *International Conference on Computer Graphics and Interactive Techniques.* New York: ACM, 1984. 213-222.

Jensen, Henrik Wann. “Global Illumination Using Photon Maps.” *Proceedings of the eurographics workshop on Rendering techniques '96.* London: Springer-Verlag, 1996. 21-30.

Jimenez, Jorge, Veronica Sundstedt, and Diego Gutierrez. "Screen-Space Perceptual Rendering of Human Skin." *Applied Perception in Graphics and Visualization.* Chania, Greece: ACM, 2009.

Kajalin, Vladimir. "Screen-Space Ambient Occlusion." In *ShaderX7*, by Wolfgang Engel, 413-424. Boston, MA: Course Technology, 2009.

Kozlowski, Oscar, and Jan Kautz. "Is Accurate Occlusion of Glossy Reflections Necessary." *Applied Perception in Graphics and Visualization.* Tubingen, Germany: ACM, 2007. 91-98.

McNamara, Ann. "Exploring Visual and Automatic Measures of Perceptual Fidelity in Real and Simulated Imagery." *ACM Transactions on Applied Perception* (ACM) 3, no. 3 (July 2006): 217-238.

McNamara, Ann. "Visual Perception in Realistic Image Synthesis." *Computer Graphics Forum* 20, no. 4 (2001): 211-224.

Mittring, Martin. "Finding next gen: CryEngine 2." *International Conference on Computer Graphics and Interactive Techniques.* San Diego: ACM, 2007. 97-121.

Möller, Tomas Akenine, Eric Haines, and Naty Hoffman. *Real-Time Rendering.* Wellesley, Massachusetts: A K Peters, Ltd., 2008.

Palmer, Stephen E. *Vision Science - Photons to Phenomenology.* Cambridge, Massachusetts: The MIT Press, 1999.

Ritschel, Tobias, Thorsten Grosch, and Hans-Peter Seidel. "Approximating Dynamic Global Illumination in Image Space." *Symposium on Interactive 3D Graphics.* Boston: ACM, 2009. 75-82.

Robertson, Barbara. “CG Society.” *Shades of Davy Jones.* 22 December 2006. http://features.cgsociety.org/story_custom.php?story_id=3889 (accessed May 15, 2010).

Shanmugam, Perumaal, and Okan Arikan. "Hardware Accelerated Ambient Occlusion Techniques on GPUs." *Symposium on Interactive 3D Graphics.* Seattle: ACM, 2007. 73-80.

Sundstedt, Veronica, Diego Gutierrez, Oscar Anson, Franscesco Banterle, and Alan Chalmers. "Perceptual Rendering of Participating Media." *ACM Transactions on Applied Perception.* ACM, 2007.

Wang, Rui, Kun Zhou, Minghao Pan, and Hujun Bao. “An Efficient GPU-Based Approach for Interactive Global Illumination.” *International Conference on Computer Graphics and Interactive Techniques.* New Orleans, Louisiana: ACM, 2009.

Yu, Insu, et al. "Perceptual Influence of Approximate Visibility in Indirect Illumination." *Applied Perception in Graphics and Visualization.* Chania: ACM, 2009.

Zhukov, Sergei, and Andrei Iones. “An Ambient Light Illumination Model.” *9th Eurographics Workshop on Rendering*, 1998: 45-56.